Aus der

Neurologischen Universitätsklinik Tübingen

Abteilung Neurologie mit Schwerpunkt neurovaskuläre Erkrankungen

EEG-triggered TMS of dorsomedial prefrontal cortex selectively modulates working memory performance depending on the phase of endogenous theta oscillation

**Inaugural-Dissertation
zur Erlangung des Doktorgrades
der Medizin**

der Medizinischen Fakultät
der Eberhard Karls Universität
zu Tübingen

vorgelegt von

Dörre, Sara Katharina

2023

Contents

List of Figures

List of Tables

List of Abbreviations

ANOVA   analysis of variance.

APB   abductor pollicis brevis.

dlPFC   dorsolateral prefrontal cortex.

dmPFC   dorsomedial prefrontal cortex.

EEG   electroencephalography.

EMG   electromyography.

EPSP   excitatory postsynaptic potential.

FDI   first dorsal interosseus.

FM-theta   frontal midline theta.

IPSP   inhibitory postsynaptic potential.

LCMV   linear constrained minimum variance.

lme   linear mixed-effects.

LTD   long-term depression.

LTP   long-term potentiation.

MEP   motor evoked potential.

MRI   magnetic resonance imaging.

MS   multiple sclerosis.

OCD   obsessive compulsive disorder.

OfC   orbitofrontal cortex.

PFC   prefrontal cortex.

PTSD   post-traumatic stress disorder.

RMT   resting motor threshold.

rTMS   repetitive transcranial magnetic stimulation.

SD   standard deviation.

TBS   theta-burst stimulation.

TMS   transcranial magnetic stimulation.

UDP   user datagram protocol.

vlPFC   ventrolateral prefrontal cortex.

vmPFC   ventromedial prefrontal cortex.

1 Introduction

1.1 General Introduction

Transcranial magnetic stimulation (TMS) is a non-invasive brain stimulation technique that uses electromagnetic induction to stimulate the cerebral cortex. TMS has been utilized in medicine for at least 30 years since the late 1980s. Initially, it was used to map brain functions anatomically by disrupting brain activity of small brain regions and to observe behavioral changes. TMS has since accrued various applications, mainly in the field of neurology and psychiatry, with both diagnostic and therapeutic uses. It can be utilized to test the functional integrity of corticospinal pathways or determine the excitability of different brain areas. For example, TMS is a valuable component in the diagnosis of multiple sclerosis (MS) and motor neuron diseases. For the therapeutic uses of TMS, an assembly of TMS specialists across the world summarized recommendations in a guideline [Lefaucheur et al., 2020]. Definitive effects for TMS treatment could be demonstrated for depression, chronic pain and stroke, as well as probable effects for Parkinson's disease, fibromyalgia, MS and post-traumatic stress disorder (PTSD) [Lefaucheur et al., 2020]. As an example, for depression, the current protocol of high-frequency repetitive TMS targets the left dorsolateral prefrontal cortex (dlPFC) [Deutsche Gesellschaft Für Psychiatrie, Psychotherapie Und Nervenheilkunde (DGPPN) et al., 2017]. For this protocol, current response rates are at 20-30 % [Avery et al., 2008; George, Lisanby, et al., 2010;

O'Reardon et al., 2007]. Although the possibility of promoting significant clinical improvement for patients with refractory depression is a considerable benefit of TMS, there is still potential for further improvement in response rates.

Over the last few years, different strategies have been identified to potentially optimize the efficacy of TMS treatment in depression, such as bilateral stimulation, treatment duration, or stimulation intensity [Cole, A. L. Phillips, et al., 2022; Cole, Stimpson, et al., 2020; Daskalakis et al., 2008]. The stimulation of cortical targets other than the dlPFC has also been considered, such as the dorsomedial prefrontal cortex (dmPFC) [Downar et al., 2013]. Another aspect contributing to low response rates is the high inter-individual variability of non-invasive brain stimulation [Hamada et al., 2012; Lopez-Alonso et al., 2014].

Some studies have found different effects of repetitive transcranial magnetic stimulation (rTMS) depending on the impact of different drugs, more specifically, effects on motor excitability due to drug intake [Ziemann, Reis, et al., 2015]. Other studies have found different effects of rTMS when the stimulation was done during the execution of tasks compared to ensuing tasks [Hill et al., 2016].

Another aspect leading to differences in the effectiveness of TMS by indicating changes in cortical excitability is the state of the ongoing local oscillations [Ridding et al., 2010]. Studies on animals and animal preparations suggest a link between ongoing brain oscillations and the evoked responses in brain activity [Arieli et al., 1996; Huerta et al., 1995; Huerta et al., 1993]. These studies demonstrate that depending on the phase of the ongoing oscillation, a stimulation may cause different or even opposite changes in excitability.

It is, however, challenging to exactly time a non-invasive stimulation to oscillatory brain activity in real-time. It requires signal processing in real-time within milliseconds. Additionally, the stimulation technique must be capable of applying pulses within microseconds and without latency while also being spatially precise. Non-invasively, this

is only possible with TMS [Hallett, 2000; Müller-Dahlhaus et al., 2013].

This thesis presents a method to face these challenges. A real-time electroencephalography (EEG)-triggered TMS design, with millisecond resolution, was used to stimulate the dmPFC. In this approach, the stimulation is synchronized to the phase of the theta oscillation originating from the dmPFC. The experiments resulted in different modulations of a cognitive function that depends on the dmPFC as a function of the targeted phase.

The following will clarify what working memory is, its relevance in behavior and disease, how to assess it, the physiological mechanisms behind working memory, and how TMS can be applied to modulate it. Subsequently, there will be details on TMS, including its mechanisms of action and the relevance of phase-specific stimulation. The chapter closes with an explanation of the aim of our experiment.

1.2 Working Memory

Working memory is a cognitive psychology concept that involves a memory system responsible for temporarily storing information while simultaneously processing and altering it. This makes working memory a critical concept for higher cognitive functions, also called executive functions, including problem-solving, interference-control, planning, and logical reasoning [Diamond, 2013; Grafman, 1995]. While several models of how working memory operates as a system exist, the most established one is described by Baddeley et al. [Baddeley, 2000]. It consists of a control system, the central executive, with three subordinate systems: the "phonological loop", the "visuospatial sketchpad", and the "episodic buffer". The "phonological loop" can be compared to an audiotape for verbal and acoustic information, running on repeat and, consequently, temporarily storing auditory information and processing it. The "visuospatial sketchpad" is a device for the maintenance, processing, and modifying of

visual and spatial information. The "episodic buffer" acts as a storage for sequences containing information from different systems, such as the long-term memory, as well as from the other subordinate systems of the working memory.

Recently, different so-called state-based models have increasingly gained significance [D'Esposito et al., 2015]. The most well-known of these models contains two separate states of short-term memory [Cowan, 1998]. The authors describe a "focus of attention" state that is capacity-limited and an "activated long-term memory", with a more extensive capacity. In the "focus of attention" state, four items of information can be held in the working memory. When shifting the attention to different items, the previous ones convert transiently into the "activated long-term memory", which is not limited in capacity but disintegrates over time.

Working memory functions, especially executive functions, have long been recognized as functions of the prefrontal cortex (PFC) [Bauer et al., 1976; Courtney et al., 1997; M. H. Miller et al., 1972]. The PFC is the front part of the brain's frontal lobe and can be subdivided into different regions. Most commonly it is divided by functionality into
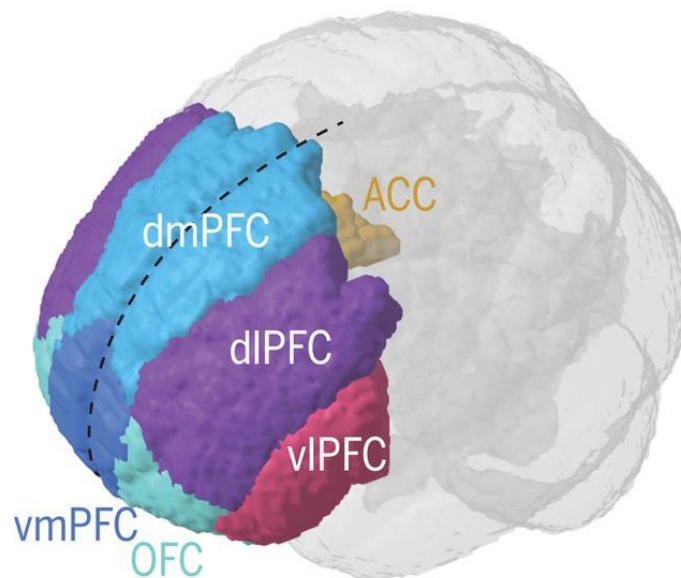

Figure 1.1: Anatomy of the PFC and its subregions.
[Image source: Carlén, 2017]

the dorsolateral prefrontal cortex (dlPFC), the dorsomedial prefrontal cortex (dmPFC), the ventrolateral prefrontal cortex (vlPFC), the ventromedial prefrontal cortex (vmPFC), and the orbitofrontal cortex (OfC) [Carlén, 2017].

The dmPFC is located in the frontal midline of the dorsal PFC. It has a variety of functions, as it is considered to be involved in emotional regulation, attention, goal-oriented behaviors, working memory, and decision-making, among others [E. K. Miller et al., 2001; M. L. Phillips et al., 2008; Venkatraman et al., 2009]. Due to the relevance of working memory in cognitive functions, its impairment can lead to significant limitations in functionality and quality of life. Indeed, depression and various other neurological and psychiatric disorders, like anxiety, obsessive compulsive disorder (OCD), schizophrenia, Huntington's disease, Parkinson's disease, bipolar disorder, and PTSD are associated with working memory impairment, which leads to a substantial impact on a patients' livability [Barch et al., 2003; Lawrence, 1998; McLoughlin et al., 2022; Reppermund et al., 2008; Wu et al., 2008]. Therefore, working memory improvement is a widely used parameter for research regarding non-invasive brain stimulation as a treatment for depression. Treatments that lead to working memory improvement may also lead to significant clinical improvement and benefit the quality of life.

1.2.1 Testing Working Memory

Various working memory tests can be subdivided into groups depending on which component of working memory is to be tested. There is semantic working memory and visual/spatial working memory. These components can be tested in their function of retention, i.e., memorizing and retrieving information after a retention period, or in their function of processing capability, i.e., analyzing or altering received information [Dehn, 2015].

Semantic Memory Retention

Semantic memory retention can be tested, for example, with letters, words, or numbers that are presented auditorily and have to be memorized. After a retention period, participants are asked to retrieve the items or are quizzed whether the list of items included a particular one [Penney, 1989].

Semantic Memory Processing

Tasks designed for testing semantic processing capability are, for example, tasks that require the categorization of auditorily presented items or verbal fluency tasks, where the participant has to name words with a selected initial [Costafreda et al., 2006].

Visual/Spatial Retention

Visual or spatial retention can be tested by the memorization of multiple images. It could involve recalling the locations of stimuli presented on a screen or a string of letters or numbers like, for example, in the Sternberg task [Sternberg, 1966; Sternberg, 1969]. For further details on the Sternberg task, see Section 2.3.5

Visual/Spatial Processing

Testing visual processing can require categorizing information, sorting it, for example, alphabetically, or detecting incongruities between pictures [Ganis et al., 2003]. A task for spatial processing could be, for example, a maze task.

Working-memory tasks can test one of these components separately or multiple components combined. The widely used n-back task [Kane et al., 2007] is an example of a task that tests multiple components. It combines testing visual retention and executive function. For this task, participants must memorize letters or numbers in sequential order and respond if a probe is the same as the letter or number n items before. This probe then has to be added to the sequence and is followed by the next

probe. While this task focuses on the retention of information, it also includes the necessity for participants to constantly update the contents of their working memory and switch their focal attention.

1.2.2 Neurophysiology of Working Memory

Our brain contains a massive network of neurons, electrically excitable cells, that communicate via synapses. The conduction of excitation along neurons works through electrical stimuli, so-called action potentials, while excitation transmission between neurons occurs via chemical substances through synapses. The chemical substances, also called neurotransmitters, can either excite or inhibit the postsynaptic neuron by opening different ion channels. Thereby, the resting membrane potential either becomes positive (depolarization) or more negative (hyperpolarization) temporarily and thereby either resulting in an excitatory postsynaptic potential (EPSP) or an inhibitory postsynaptic potential (IPSP). Once the depolarization reaches a certain threshold, an action potential is triggered, which is then passed on through the axon to other connected neurons. If the threshold is not reached, the neuron stays depolarized, resulting in higher excitability for some time. A hyperpolarization, however, results in lower neuron excitability for further stimuli.

Neurons do not work as single units. They are organized in networks and create rhythmic patterns of activity, the neural oscillations. When multiple neurons of a region act synchronously, they create an electric current by fluctuations of ion concentrations in the extracellular compartment due to their cellular activity, resulting in extracellular field potentials.

Different brain regions are hypothesized to communicate by synchronizing their oscillations, thereby participating in different functional networks. These networks are constantly being reorganized and, thereby adapt to changing cognitive demands

[Buzsáki et al., 2004; Fell, Klaver, et al., 2001]. Through synchronized activity between a selected presynaptic neuronal group and a postsynaptic group, it is also possible to achieve selective communication, which is critical for neuronal processing [Fries, 2015].

Oscillations can be recorded with scalp EEG. Here, electrodes placed on the scalp measure local changes in voltage. The recorded oscillations are classically divided into different frequencies and are segmented into frequency bands: delta (1-4 Hz), theta (4-8 Hz), alpha (8-12 Hz), beta (13-30 Hz), and gamma (30-80 Hz). The multiple frequency bands are believed to be related to particular brain regions and functions. Due to its relevance in working memory, we focused our study on the theta oscillation. Therefore, it will be discussed in more detail in the following, including its relevance to working memory.

Theta Oscillation

There are several types of theta rhythms in the brain originating from specific regions and associated with distinct behavior.

The theta oscillation was first and most extensively described in the hippocampus. The hippocampus is a structure responsible for long-term memory formation located in the medial temporal lobes. The hippocampal theta rhythm is related explicitly to spatial navigation, attention, working memory, and, by influencing synaptic plasticity, long-term memory. Different phases of hippocampal theta oscillation seem to be associated with different states of excitability, with neuronal spiking concentrating on selected phases of the theta oscillation [Benchenane et al., 2010; Fujisawa et al., 2011]. Furthermore, Rutishauser et al. could demonstrate that spikes of neuronal activity coordinated with hippocampal theta oscillation determines the effectiveness of memory formation [Rutishauser et al., 2010].

Additionally, the hippocampus cooperates with different brain regions, for example, the PFC. It has been shown that neurons of the medial PFC phase-lock to the hippocampal theta oscillation [Siapas et al., 2005]. This mechanism is believed to contribute to cognitive tasks, such as working memory, by coordinating interactions between the dmPFC and the hippocampus [Colgin, 2011].

This work focuses on a different type of theta oscillation, the frontal midline theta (FM-theta) rhythm, which is generated by the medial PFC [Ishii et al., 1999]. It has been widely reported to occur during working memory tasks and seems to be active in memory maintenance with increased power for higher working memory loads [Gevins, 1997; Hsieh and Ranganath, 2014; Jensen and Tesche, 2002; Onton et al., 2005; Sarnthein et al., 1998; Schacter, 1977]. Therefore, the FM-theta is believed to be essential for working memory retention, among other functions. Additionally, it is associated with episodic memory encoding and retrieval as well as cognitive control [Cavanagh, M. X. Cohen, et al., 2009; Cavanagh and Frank, 2014; Klimesch, Doppelmayr, et al., 1996; Klimesch, Hanslmayr, et al., 2005]. Moreover, McLoughlin et al. investigated how different oscillatory dynamics of theta differ in patients with psychiatric conditions linked to an impairment in cognitive control [McLoughlin et al., 2021].

Furthermore, there is a physiological mechanism associated with theta oscillations in general, through which the functions mentioned above are realized. Theta oscillations are essential in organizing brain activity and learning processes by utilizing phase-locking mechanisms to induce synaptic plasticity [Siapas et al., 2005].

Synaptic Plasticity

An essential foundation of learning processes is synaptic plasticity. It is postulated that memories are stored by an alteration of synaptic connections and changes in the number of synapses [Cajal, 1894; Konorski, 1948].

Synaptic plasticity describes the capability of the brain to rewire itself by remodeling synaptic connections between neurons. For example, the synaptic connections can transform by the alteration of ion channels. Additionally, synaptic plasticity can be achieved through the different mechanisms of long-term potentiation (LTP) and long-term depression (LTD). Synapses typically respond to high-frequency activation with LTP by sustaining an increased excitability for further activation [Bliss and Collingridge, 1993; Bliss and Lomo, 1973]. To a prolonged low-frequency stimulation, synapses typically respond with LTD and, thereby, are less excitable [Mulkey et al., 1992].

LTP and LTD can also be achieved by synchronizing oscillations [Axmacher et al., 2006; Jutras et al., 2010]. This coupling of oscillations occurs naturally in the brain either as phase-amplitude or phase-phase coupling. It could be observed persistently during information maintenance for working memory tasks and information encoding [Payne et al., 2009; Sato et al., 2007].

Cross-frequency phase-amplitude coupling is a mechanism by which the phase of slower oscillations affects a faster oscillation's amplitude, as visualized in Figure 1.2. It results in rhythmic bursts of the higher frequency oscillation adjusted to the phase of the lower frequency oscillation. Especially the phase-amplitude coupling between theta and gamma oscillations could be observed during working memory tasks and processing and retrieval of information [Fell and Axmacher, 2011]. It is argued that the mechanics of this theta-gamma phase-amplitude coupling can explain the limitations of working memory storage. According to this model, each gamma cycle encodes a single working memory item. Given the limited number of gamma cycles that can be nested
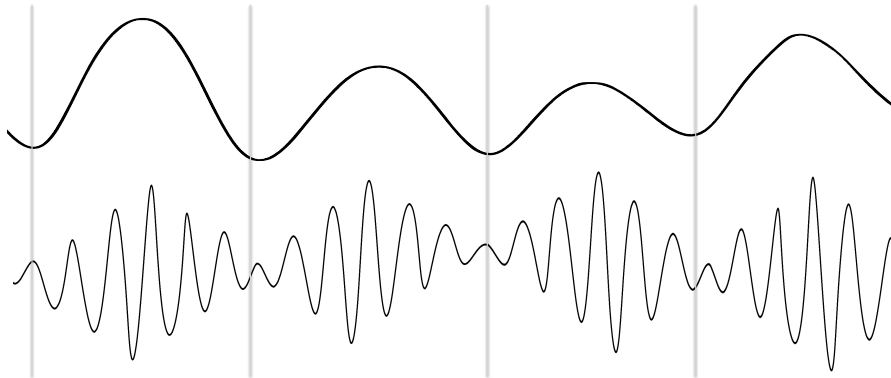
Figure 1.2: Schematic illustration of the phase-amplitude coupling mechanisms. The lower frequency oscillation at the top of the diagram shows a phase-amplitude coupling with the higher frequency oscillation.
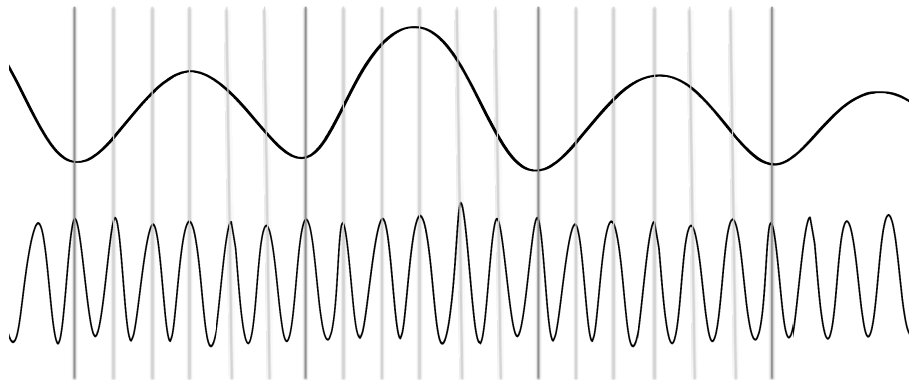
Figure 1.3: Schematic illustration of the phase-phase coupling mechanisms. The high-frequency oscillation at the bottom shows a phase-phase coupling with the lower frequency oscillation.

within a theta cycle, a quantitative limit of items one can store in working memory is dictated [Jensen and Lisman, 2005]. Ultimately, this model ties the neurophysiological observation of theta-gamma coupling to behavioral functioning.

Oscillations of different frequencies can also be synchronized in their phases, which is called cross-frequency phase-phase coupling, see Figure 1.3. Here, one phase of the cycle of the higher frequency oscillation can be synchronized to specific phases of the lower frequency oscillation. For example, the eight cycles of gamma oscillation

that fit temporally within one cycle of theta oscillation synchronize their peak to eight different phases of one theta cycle (for further explanation, see [Fell and Axmacher, 2011]). This mechanism could also be observed during working memory maintenance with theta-alpha coupling and theta-gamma coupling [Sauseng et al., 2009; Schack et al., 2005].

1.3 Transcranial Magnetic Stimulation

Transcranial magnetic stimulation (TMS) is a non-invasive technique to stimulate the brain through the intact scalp. There are two general options for non-invasive induction of current in the brain. On the one hand, there is the method of applying direct current through the scalp, which includes modalities such as transcranial direct current stimulation, transcranial alternating current stimulation, and electroconvulsive therapy, among others. On the other hand, there is the method of inducing current via a magnetic field with TMS.

In the case of magnetic stimulation, the electric potential difference is induced via a magnetic field according to Maxwell-Faraday's law of induction. An electric current flowing through a wire generates an orthogonal magnetic field. If now the current flow of the coil is changed over time, the magnetic flow also changes over time. This creates an electric field and subsequent flow of current in conductive tissues.

The magnetic coils used for stimulation consist of multiple loops of wire. There are different types of coils with specific characteristics. Initially, circular coils were used, which have a broad action radius with a ring-shaped stimulation area. This makes precise stimulation of smaller areas difficult. Figure-of-eight coils are used for a more focal application due to their small stimulation zone. The focality of the stimulation is achieved by having two connected circular coils that work in opposite directions. The two induced electric fields add up at their point of contact.

The magnetic coil is placed tangential to the scalp for the stimulation, generating a magnetic field perpendicular to the scalp. Consequently, an electric field is created that is oriented horizontally to the scalp. The generated current flow in the tissue runs parallel to the current flow in the coil but in the opposite direction.

In order to achieve activation of neurons, the stimulation has to shift the resting membrane potential in the form of a supra-threshold depolarization, through which an action potential is triggered. The decisive factor for this is a high spatial gradient of the electric field in relation to the course of the axon. A spatial gradient is a rate of change of the field strength along a spatial direction. A high spatial gradient can be achieved in different ways. One possibility is that the axon is straight and runs parallel to the field. Here the highest gradient is located where the intensity of the field changes as a function of distance.

Another possibility would be that the axon bends at some point, which also results in a high electric gradient at this point. This electric gradient causes a transmembrane current flow, whereby an inwardly directed flow of sodium ions occurs through sodium ion channels into the cell, leading to depolarization, as desired. If this depolarization surpasses a certain threshold, voltage-dependent sodium ion channels open with the result of an action potential, which is then conducted through the axon. Through the connections of the activated neurons, the induced excitation can consequently modulate the excitability of the stimulated brain area, leading to an increased or decreased excitability while also influencing connected brain areas. Whether the stimulation facilitates or inhibits brain excitability depends on the stimulation frequency [Fregni et al., 2007; George and Aston-Jones, 2009; Hallett, 2007].

The stimulation intensity is a further technical aspect of TMS. Since the intensity needed to evoke an action potential varies between patients, coils, and stimulation devices, it should be determined individually, using the parameter of the resting motor threshold (RMT). How its value is determined is explained in Section 2.3.3.

Using the phenomenon of magnetic induction has advantages as opposed to directly creating an electric field via electrodes. For achieving a depolarization in cortical neurons, TMS is virtually pain-free, unlike direct current stimulation. While brain tissue and skull represent a significant electric resistance, requiring a higher voltage when applied to the scalp directly, a magnetic field is nearly undiminished when passing through the skull or other non-conductive tissue. Additionally, the electrodes for an electric stimulation directly activate pain receptors by generating high current densities at the site of skin contact. However, the magnetic field and, therefore, the electric field decreases rapidly with the distance from the coil. This limits the depth range of magnetic stimulation to a few centimeters depending on the utilized coil type.

In order to have a lasting therapeutic use, the stimulation needs to be able to induce changes that outlast the stimulation itself. This is possible through the induction of synaptic plasticity.

1.3.1 Plasticity Effects of TMS

When TMS is applied with trains of pulses at a defined pattern, it is also called repetitive transcranial magnetic stimulation (rTMS). Experimental findings suggest that rTMS can induce lasting effects through LTP-like mechanisms [Ziemann, Paulus, et al., 2008]. The mechanism behind this has been investigated at a cellular level on in vitro models of entorhino-hippocampal slice cultures from mice [Vlachos et al., 2012]. Here, repetitive magnetic stimulation resulted in long-lasting increased synaptic strength by accumulating a specific type of glutamate receptors.

Another method targeting to improve the induced plasticity is the theta-burst stimulation (TBS) [Huang et al., 2005]. This is a stimulation protocol of rTMS, where bursts of triple-pulses with a frequency of 50 Hz are delivered repetitively at 5 Hz, which is within the theta frequency band of 4-8 Hz, with or without pauses as continuous

or intermittent TBS. This patterned protocol was designed because of the distinct role of the theta oscillation in plasticity, as mentioned before, mimicking the theta-gamma coupling phenomenon, which is associated with increased neuroplastic effects. The method was verified to be superior in inducing LTP compared to other forms of stimulation [Larson et al., 2015]. Regardless, TBS protocols could not demonstrate a significant benefit in their behavioral outcome compared to the standard rTMS method [Blumberger et al., 2018]. One possibility is that although it simulates the physiological theta-gamma coupling phenomenon, it does not consider the ongoing cortical oscillation and current brain state.

1.3.2 Phase-Dependent Stimulation

The concept of a phase-dependent stimulation is visualized in Figure 1.4. The current brain state is measured by the EEG. The measured data are consecutively filtered and analyzed by an algorithm to estimate the ongoing phase of a selected oscillation. With the estimated phase, stimulation can be triggered to occur at a specific phase. Through the applied stimulation, the current brain state can, in turn, be modulated.
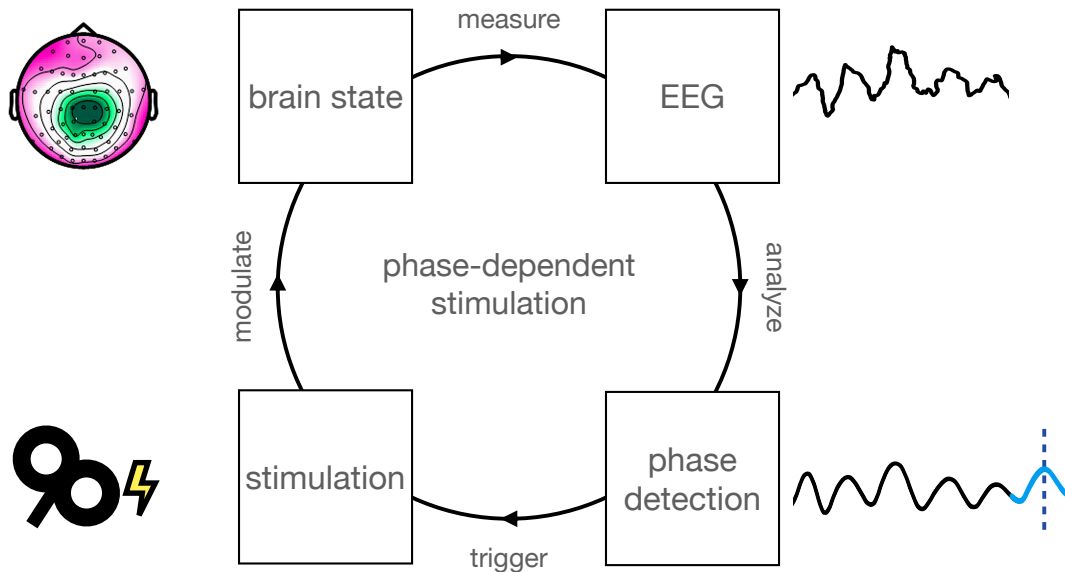
Figure 1.4: Illustration of the concept of phase-dependent stimulation with its different components. [Figure inspired by Bergmann et al., 2016]

For our experiment, the different steps necessary for the developed method of a theta phase-dependent stimulation are the following:

1. Recording of resting-state EEG and other measurements of brain state/excitability and behavior (with the Sternberg task) before stimulation

2. Filtering of resting-state EEG signal (individual spatial filters to extract the dmPFC 's theta oscillation)

3. Phase estimation of the filtered signal

4. Triggering of TMS pulses dependent on the ongoing estimated phase (with some restrictions)

5. Measurements of modulations in brain state/excitability and behavior after stimulation

Research investigating the relevance of timing of applied stimulation, dependent on the current brain state, concludes that the phase of ongoing oscillations corresponds to high or low excitability and determines the direction of synaptic plasticity. Zrenner et al. used TMS on the motor cortex, phase-locked to sensorimotor μ-alpha rhythm, to induce plasticity effects [Zrenner, Belardinelli, et al., 2017a; Zrenner, Belardinelli, et al., 2017b]. They showed that bursts of high-frequency (100 Hz) stimulation applied to the μ-alpha rhythm, i.e., the dominating rhythm in sensorimotor cortex, resulted in increased motor cortical excitability for up to 30 minutes after the intervention. Concerning theta phase-specific stimulation, a study on in-vitro hippocampal slices of rats could demonstrate either LTP or LTD ensuing a theta phase-specific stimulation [Huerta et al., 1995; Huerta et al., 1993]. In anesthetized rats, Pavlides et al. demonstrated that stimulation applied at the peak of an induced theta rhythm generated LTP while stimulation at the trough decreased excitability [Pavlides et al., 1988]. In conclusion, the mentioned research suggests that different phases of ongoing theta or alpha rhythms correspond to different excitability states of neuronal units.

Moreover, Berger et al. could show on healthy human subjects that a stimulation performed simultaneously to a working memory task resulted in differences in accuracy in the task depending on the stimulated phase [Berger et al., 2019]. However, the phases were not explicitly targeted but analyzed post hoc and assigned to the trials performed during the stimulation. Nevertheless, this research provides a solid foundation upon which our experiment can build by demonstrating that the reported observations are not sole correlations but can be directly produced or causally manipulated.

1.4 Aim of the Study

The objective of this study was to determine whether a phase-specific stimulation, either targeting the trough or peak instead of a random phase, of the ongoing theta rhythm in the dmPFC results in differential modulation of working memory performance. Using a phase-locked stimulation, we attempt to imitate the mechanism of phase-amplitude coupling. Specifically, we use high-frequency triple bursts of stimulation synchronized to a selected phase of theta, thus, practically generating an artificial theta-gamma phase-amplitude coupling. We hypothesize that this specifically targeted stimulation is closer to the actual naturally occurring processes in the brain and, therefore, superior to random stimulation, which has previously been used to influence working memory. We investigated whether stimulation applied to either the positive peak or the trough of the endogenous theta oscillation of the dmPFC is superior to random stimulation in affecting working memory performance.

Based on the mentioned previous research, we hypothesize that phase-specific TMS applied to either the positive peak or the trough of the endogenous theta oscillation of the dmPFC has different effects on working memory performance and is superior to random phase stimulation.

2 Material and Methods

2.1 Experimental Procedure

The experiment consisted of four sessions for each participant. Figure 2.1 illustrates the procedure for the first session, while Figure 2.2 presents an overview of the design for the three remaining sessions. The first session was performed to collect different measurements. Among other measurements, the RMT was determined in this session, as well as the calculation of each subject's spatial filter. The purpose and methods involved in this spatial filter will be discussed below in Section 2.3.4. Additionally, a second resting-state EEG was recorded for an analysis of the accuracy of the phase estimation, which will be discussed in Section 2.4.2.

Regarding the remaining three sessions, each session contained a phase-dependent triple-pulse intervention. Measurements were recorded both before and after this intervention. Each session started with the recording of eight minutes of resting-state EEG, followed by stimulation with both a sham, i.e., a "fake" stimulation, and a real TMS coil, with single pulses at 120% of the RMT. This was done to assess the excitability of the dmPFC,by measuring changes in the EEG ensuing TMS pulses. As for the measurements before the intervention, stimulation with the sham coil was executed first. The measurement block after the intervention was the other way around. The last element of the measurements was the Sternberg task with 100 trials.

After completing the first block of measurements, the intervention was conducted. It

Excitability Session (Session 1)

Measurements:

Resting state EEG

Resting state EEG for collecting markers

Determination of RMT and generation of spatial filter

DMPFC Excitability (phase dependent):

- 480 single **TMS** pulses (120% RMT)
  With each stimulation randomly at one of the three different conditions:
  theta-peak / theta-trough / random phase
  (160 pulses each)

- 480 single **Sham** pulses (120% RMT)
  With each stimulation randomly at one of the three different conditions:
  theta-peak / theta-trough / random phase
  (160 pulses each)

Figure 2.1: Overview of the first session for each participant.

consisted of 400 triple pulses of a phase-dependent stimulation with the TMS coil at 100% of the RMT. The triple pulses were applied with a frequency of 100 Hz. For each of the three sessions of the experiment, the targeted stimulation phase was either at the theta oscillation peak, its trough, or a random phase for control. The order of these sessions was randomized and, therefore, unknown to the subjects. Following the intervention, the same measurements were recorded as before.

This thesis focuses on the measurements of the working-memory task. The analysis of the excitability of the dmPFC was the topic of a different hypothesis and is, therefore, not included in this work. Consequently, an explanation of how the sham stimulation

Plasticity Sessions (Sessions 2-4)

Measurements before intervention:

Resting state EEG

DMPFC Excitability (not phase dependent):
- 160 single **Sham** pulses (120% RMT)
- 160 single **TMS** pulses (120% RMT)

Sternberg **working-memory task**: 100 trials

Intervention (phase dependent):

400 triple TMS pulses (100% RMT)
Stimulation either at:
   theta-peak / theta-trough / random phase

Measurements after intervention:

Resting state EEG

DMPFC Excitability (not phase dependent):
- 160 single **TMS** pulses (120% RMT)
- 160 single **Sham** pulses (120% RMT)

Sternberg **working-memory task**: 100 trials

Figure 2.2: Overview of the experimental procedure for the remaining three sessions. Each subject participated in three of these sessions, during which the phase-dependent stimulation occurred at a different phase of the theta activity coming from the dmPFC. The sequence of these sessions was randomized and unknown to the subjects.

was conducted is also not included. However, for more details on the methods and results of the measured TMS evoked potentials, see [Gordon, Belardinelli, et al., 2022].

In the following, the composition and selection of our participant group will be described, succeeded by an explanation of the different elements and methods required for the realization of our experiment. Finally, a description of the performed data analysis is presented.

2.2 Subjects

Right-handed ($\geq$ 75% on the Edinburgh Handedness Inventory [Oldfield, 1971]) subjects aged between 18 and 50 years in good physical and mental health were included in the study. Female Participants were required to use a hormonal method of contraception.

Exclusion criteria included a history of neurological or psychiatric disorders. The intake of drugs or excessive caffeine consumption was also considered as exclusion criteria, as well as working night shifts. Participants with a condition precluding the execution of an MRI or ones refusing to be informed in case of accidental pathological findings on MRI were excluded. Subjects were excluded if there was any concern by the investigator regarding the safe participation of a subject in the study or for any other reason the investigator considered the subject inappropriate for participation in the study. Before the first study visit, subjects could not participate in another study for two weeks and throughout the study.

While 20 subjects participated in the experiment, only 16 were able to complete the whole experiment successfully. Two participants had to be excluded due to sleepiness during study sessions, and two additional participants were excluded because of excessive eye movements and muscle contractions during the experiment.

A total of 16 healthy individuals, ten females and six males completed our study. The mean age of all subjects was 23.4 years ($\pm$ 3.3 standard deviation (SD))

None of the subjects reported any side effects or discomfort during or after stimulation.

Prior to participating, all subjects supplied written consent to participate voluntarily in the trials and confirmed to have been informed about possible risks of the study. For their expenses, participants were financially compensated. The study was approved by the local ethics committee of the medical faculty of the Eberhard Karls University of Tübingen (Project number: 716/2014BO2) and complies with the Declaration of Helsinki.

2.3 Experimental Setup and Preparation

Sessions of the experiment took place in an enclosed, quiet room. Participants of the study were seated on an upholstered, reclined chair for the entire duration of each session with a computer screen in front of them at a distance of one meter. They were asked to stay awake and keep their eyes open for each measurement and stimulation. A vacuum cushion was offered to help keep their head in the same position during stimulation episodes.

The setting is illustrated in Figure 2.3. Figure 2.3a shows a participant performing the working memory task. The screen displays ten consonants that need to be memorized for the ongoing trial of the task. For further explanations concerning the task, see Section 2.3.5. The subject is holding a device with four buttons for answering at a later time when the cue is displayed. For ergonomics, there are two buttons respectively for answering "yes", i.e., the displayed set included the cue or "no", i.e., the cue was not included, arranged with different spacing on the remote. The TMS coil with its corresponding marker is also on display here, but it is not attached to the participant's head as it is not used during the working memory task.

(a) Display of a participant performing the Sternberg task. The TMS coil in the image is not active during the task.

(b) Illustration of a participant during the intervention period of a session while stimulation takes place.

Figure 2.3: Demonstration of the experiment setting. A participant is sitting in a reclining chair for the experiment in front of a screen and with a vacuum cushion used to stabilize the head in a fixed position during the stimulations.

Figure 2.3b illustrates a participant during the phase-dependent stimulation. Here the TMS coil is attached to target the dmPFC during stimulation. On top of the screen in front of the subject, a camera is visible. This camera tracks the subject's head as well as the coil for the neuronavigation. The screen displays a fixation cross to help the participants fix their eyes, thereby reducing artifacts due to eye movements.

To minimize auditory evoked potentials caused by the TMS triggering noise, a masking noise was used. During stimulation, either with the sham coil or the TMS coil, subjects were wearing in-ear headphones delivering a masking noise (white noise). The volume was adjusted either to a level where the TMS triggering noise was no longer audible to subjects or the highest volume tolerable.

2.3.1 Localization of the Stimulation Target

Before the first session, magnetic resonance imaging (MRI)-scans (T1- and T2-weighted anatomical sequences) were obtained for each subject by a 3T Siemens PRISMA scanner. Having these individual MR images is a requirement for using MRI-guided neuronavigation. As a neuronavigation system, we used the system from Localite GmbH, Sankt Augustin, Germany.

To precisely stimulate the selected anatomical target, neuronavigation is an essential component for TMS. To locate certain brain regions from the outside, one has to navigate toward the exact spot where the stimulation coil needs to be placed. This process relies on individual MRI, a stereoscopic infrared camera system, and a reference marker of reflective spheres firmly attached to the subject's head. After specific markers are defined, the program can assign the individual MRI to the participant's physical head. Because the coil carries its own marker, it is recognized by the navigation system, and its location in relation to the position of the subject's head can be estimated. Thus, it is possible to place the coil precisely on the right spot and check its location throughout the stimulation. Thereby, the position of the coil can be corrected accordingly if a subject's head shifts slightly.

For source estimation of the measured signals, it was also necessary to register the position of every electrode of the EEG cap. These data were required to design the individual's spatial filter, which will be explained further in Section 2.3.4.

2.3.2 EEG

An EEG cap containing 126 electrodes was used to record high-density EEG signal, as recommended for source estimation (EasyCap GmbH, Germany). The electrodes were TMS compatible sintered ring electrodes made of silver and silver chloride. They were

arranged according to the international 10-5 EEG system (illustrated in Figure 2.5a [Oostenveld et al., 2001]. The correct size of the cap was determined by measuring the circumference of each subject's head.

Prior to each session, the EEG cap had to be placed on the participant's head and prepared. After ensuring that the cap was centered correctly, the scalp beneath each electrode was scrubbed with an abrasive paste and filled with contact gel to minimize the electrical resistance. FCz was used as a reference electrode, and AFz as a grounding electrode.

To amplify the EEG signals, a 24-bit biosignal amplifier was used (NeurOne Tesla with Digital Out Option, Bittium Biosignals Ltd. Finland). Data were recorded in DC mode with a sampling rate of 5 kHz, meaning the signal of the EEG cap was sampled and captured 5000 times per second. To put this into context, one phase of the theta oscillation was sampled approximately 1000 times. The data were simultaneously sent to a real-time processor through user datagram protocol (UDP) at a packet rate of 5 kHz (one sample per channel).

For a continuous recording of the EEG signal, the software Vision-Recorder (Brain Products GmbH (Gilching, Deutschland)) was used. In order to ensure clear signals, the software was also utilized to check and improve the impedance of all electrodes to be below 20 kΩ and for frontal electrodes below 10 kΩ. For this study, the focus was on frontal electrodes because they were essential for a precise generation of the spatial filter, as it concentrates on filtering a signal originating from the frontal part of the brain.

2.3.3 Specifics of Stimulation

For the magnetic stimulation, biphasic pulses were delivered using a figure-of-eight coil (Cool-B65, inner coil winding diameter 35 mm) to achieve focused stimulation at the predetermined area. The coil was connected to a MagPro XP Stimulator (MagVenture A/S, Denmark). To reduce possible artifacts due to direct contact of the coil to the EEG-electrodes, a plastic spacer of 11 mm thickness was placed between the EEG-cap while surrounding the electrodes and the coil whenever the coil was positioned for stimulation.

The stimulation intensity was determined by the individual RMT of every subject at the beginning of the experiments. For the measurement of the RMT, electromyography (EMG) was recorded through bipolar EMG adhesive hydrogel electrodes. EMG-electrodes were placed over the abductor pollicis brevis (APB) and the first dorsal interosseus (FDI), each with a grounding electrode placed over the bone of the finger. The EMG, like the EEG, was amplified using a 24-bit biosignal amplifier (NeurOne Tesla with Digital Out Option, Bittium Biosignals Ltd. Finland) and sampled at a rate of 5 kHz. The acquired signal was band-pass filtered at 0.16 Hz - 1.2 kHz, meaning only frequencies included in this range were regarded. The TMS-coil was positioned over the left primary motor cortex (M1) hand area to generate motor evoked potential (MEP)s, i.e., muscle activity detected by the EMG.

There are several different methods to determine the RMT. We used a standard method by Groppa et al. [Groppa et al., 2012]. This method is based on measuring the lowest intensity for which at least 5 out of 10 MEP exceeded a peak-to-peak amplitude of 50 μV.

The steps described in this section were required to establish the stimulation intensity, which was 100% of the individual's RMT for the intervention.

2.3.4 EEG-Triggered TMS

To make theta-phase-dependent stimulation possible, an instantaneous phase esti-
mation was needed. For this, it was necessary to isolate the theta oscillation of the
dmPFC with a spatial filter.

Spatial Filter

In order to extract the brain activity of the left dmPFC, the individual MRIs needed to
be segmented into cortex, scalp, and skull. The softwares used for this segmentation
were SimNIBS [Windhoff et al., 2011], FreeSurfer [Fischl, 2012], and FSL [Jenkinson
et al., 2012]. The anatomical location of the left dmPFC was identified by using MNI
(Montreal Neurological Institute) coordinates (-4, 52, 36) and marked on each subject's
cortical mesh.

For source estimation from EEG signals, spatial filters were used. The calculation
of these spatial filters was based on linear constrained minimum variance (LCMV)
beamforming [Veen et al., 1997] and included signals of all electrodes except the
ones of the outer rim (electrodes labeled 9 and 10 in the International 10-5 EEG
system). The filter was calculated using the signal covariance matrix on eight minutes
of resting-state EEG and the lead-field matrix containing the signal topographies (for
further details on the comparison of the matrices, refer to [Gordon, Dörre, et al., 2021;
Veen et al., 1997]). The topographical distribution of the recorded prefrontal theta
oscillation is presented in Figure 2.4a. This signal was analyzed to estimate the source
of the theta oscillation via beamforming, which is visualized in Figure 2.4b. The location
of interest for the beamforming was specified as dipoles within a one-centimeter radius
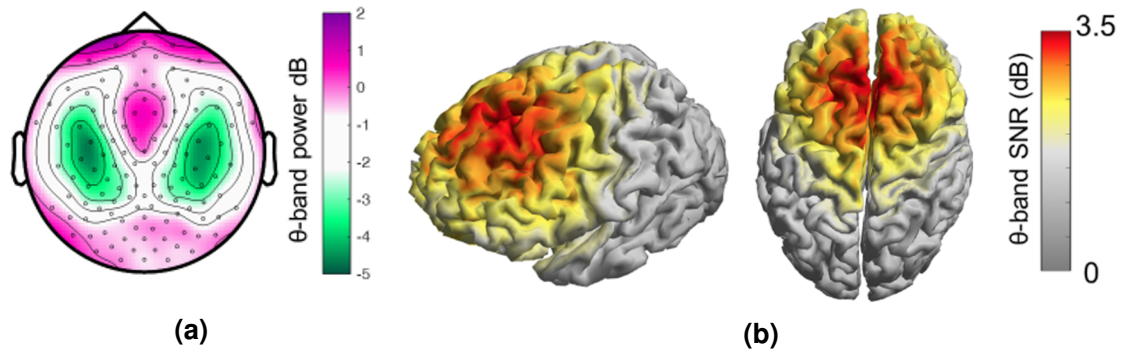of the left dmPFC.

(a)   **(b)**

Figure 2.4: Illustration of the process of creating the spatial filter via beamforming:
(a) Distribution of the spectral power of prefrontal theta oscillation illustrated over a 126-electrode EEG. The measurements were averaged from resting-state EEG of 18 subjects.
(b) Source modeling of theta oscillation and distribution of its spectral power over a cortical mesh, calculated using LCMV beamformer.
[Image source: Gordon, Dörre, et al., 2021]

The spatial filters were attuned for each subject and recalculated at every session, as they rely on the exact position of the EEG electrodes with respect to the brain and the acquired signal of the resting-state EEG.

Figure 2.5a features the proportions at which different EEG channels are considered for the spatial filter of one individual subject as an example. Figure 2.5b illustrates the distribution of the same individual's filter's sensitivity on an averaged cortical plot. The power spectrum of the filtered resting-state EEG is presented in 2.5c with a distinct peak at around 5-8 Hz, in addition to different oscillation signals at around 15-20 Hz that are located outside of the targeted frequency range.

Phase estimation

A customized digital biosignal processor based on Simulink Real-Time was used to analyze a copy of the EEG data in real-time and trigger TMS pulses depending on the phase of the theta oscillation originating from the left dmPFC. The EEG signal was analyzed in sliding windows of data with 1024 ms length (down-sampled to 250 Hz:
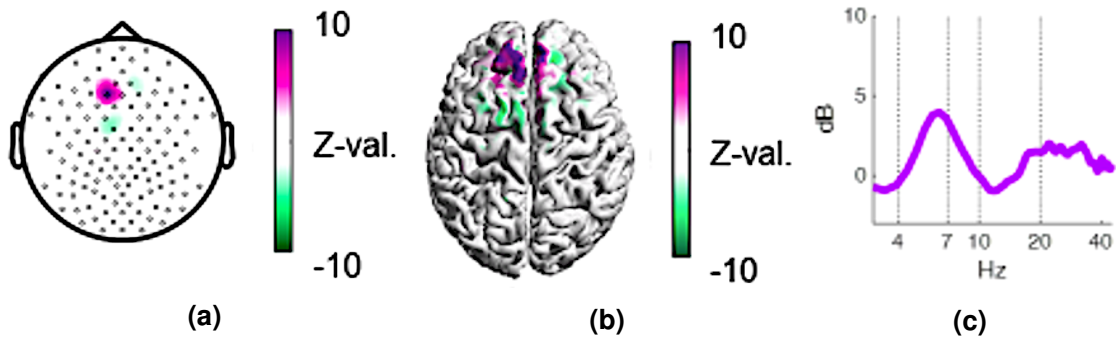
Figure 2.5: Specifics of the spatial filter of one individual subject as an example.
(a) Respective weights of different EEG channels of the spatial filter.
(b) Sensitivity profile of the spatial filter presented on an averaged cortical plot.
(c) Power spectrum of the resting-state EEG acquired through the spatial filter.
[Image source: Gordon, Dörre, et al., 2021]

256 samples). This means that the data that are being continuously analyzed have a predefined length and change over time as new samples of data are acquired. To achieve a real-time analysis, the sliding windows always consider the latest samples acquired. For each new sample, the oldest one gets replaced. Analysis of these sliding windows was performed by utilizing the following steps:

1. Band-pass filter:

The signal is filtered at 5-8 Hz (the frequency of theta) to enable phase estimation.

2. Removal of 50 samples:

Samples at the edges need to be removed to reduce filtering edge effects because these effects would considerably distort the signal and would preclude accurate phase estimation.

3. Autoregressive forward prediction:

Due to ongoing time and the removal of the 50 most current samples, the phase at the time point of interest is unknown and needs to be reconstructed. This is done using an autoregressive forward model to predict the missing signal distribution.

4. Hilbert transformation:

The resulting signal, including the actual recorded signal and the forward prediction reconstructed signal, is then converted into an analytic signal via the Hilbert transformation. The resulting phase-angles then correspond to the instant phases of the theta oscillation.

Ranges were defined where the oscillation was considered to have a positive or negative peak. They were defined at $0° \pm 6°$ and $180° \pm 6°$ radians, respectively. A TMS pulse was triggered whenever the estimated phase was within this preset range for the targeted phase. However, in certain situations, the phase estimation could be inaccurate. Therefore, the algorithm was prevented from triggering a pulse under certain conditions.

Precautions against Incorrect Triggering

There are two kinds of artifacts potentially misleading to proper phase estimation: Artifacts due to eye movement and muscle artifacts. For artifacts due to eye movement, TMS triggers were blocked for 700 ms whenever the combined signal from electrodes Fp1, Fp2, and two additional electrodes, placed between the zygomatic prominence and the lower eyelid, exceeded a certain threshold. For muscle artifacts, there was a threshold for every electrode that, if surpassed, blocked TMS triggers for the currently analyzed sliding window.

Another difficulty for phase detection is phase resetting. The endogenous theta oscillation occurs in distinct episodes with phase resetting in between and fluctuating amplitudes [Kahana et al., 1999]. Therefore, the algorithm only triggered if no phase reset was detectable for the last 500 ms to ensure a stable oscillation before initiating a stimulation. In addition, an amplitude threshold was implemented in case there was no theta oscillation present to be reliably detected.

2.3.5 Working Memory Task

A modified Sternberg task [Sternberg, 1966] was used as a working memory test both before and after the intervention. It is a classic verbal working memory retention task and consists of a memorization period, a retention period, and a query.

During the memorization period, a set of ten consonants (white letters on a black background) was presented for two seconds. This number of consonants was chosen as it provided an appropriate level of difficulty, which will be explained further in the next chapter. After a retention period of three seconds, with a black screen, a probe was displayed in the form of a single consonant. Participants were given two seconds to press either "yes" or "no", to answer whether the memorized set contained the probed
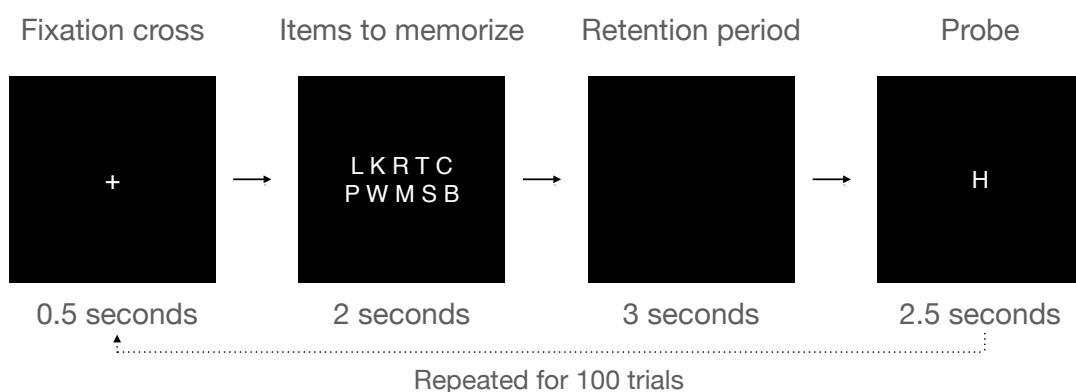

Figure 2.6: Sequence of the Sternberg task and its appearance for participants.

letter. The time it took participants to respond was measured as well as whether the given response was correct. Whenever no response was detected, the trial was counted as false without taking the reaction time into account for the analysis. After a one-second break, the next set of consonants was shown.

The task was repeated for 100 trials. For reference on how the trials looked like for participants, see Figure 2.6.

2.4 Data Analysis and Statistics

2.4.1 Power Analysis

When devising the experiment, a power analysis was conducted in order to estimate the presumably needed sample size. The result of this analysis was a sample size of 23 participants to receive significant results while assuming an effect size of 0.5 and using mean values of the mean differences and standard deviations of previous studies on TMS and working memory performance [Dedoncker et al., 2016]. The sample size (n) was calculated by using the software G*power [Faul, Erdfelder, Buchner, et al., 2009; Faul, Erdfelder, Lang, et al., 2007]. Because of the complex and time-consuming nature of the experiment, we decided to perform the study on only 16 subjects. Therefore, the study was planned as a pilot study to investigate the effects of the phase-dependent stimulation in a smaller experiment before conducting an expanded experiment.

2.4.2 Analysis of the Accuracy of the Phase Detection

In order to determine the accuracy of our phase-detection algorithm and, therefore, know how reliable the results are, a resting-state EEG was recorded, where the algorithm needed to predict the phase and set markers, but without triggering a TMS

pulse. This allowed the analysis of the accuracy of phase-detection because the separately recorded EEG data were not disrupted by an artifact created by the TMS pulse. This analysis of accuracy was conducted by determining the phase of the markers collected in each of the EEG recordings and comparing it to the estimated phase of the algorithm.

2.4.3 Analysis of the Sternberg Task

The statistical analysis of the Sternberg task was conducted using Matlab (Mathworks). The accuracy of subjects' responses was calculated by forming the fraction of correct responses from all responses.

In order to determine the general significance of the data, linear mixed-effects (lme) models were used. They are extensions of linear regression models for data organized in groups. Lme models are also similar to repeated measures analysis of variance (ANOVA), which is a variance analysis for data collected on the same subject at different time states. Unlike the repeated measures ANOVA, these models can include every observation without over-fitting the data and while taking into account different effect variables [Polti et al., 2018]. The inter-individual variability was included as a random effect variable. The phase of the condition that was stimulated during the intervention was included as a fixed effect variable.

A variance analysis, in the form of an ANOVA, was conducted on the results of the lme models for reaction times and accuracies.

A one-sample Kolmogorov-Smirnov test was applied to determine if the data were normally distributed, revealing non-normally distributed data. Therefore, for the data that showed significant interactions (ANOVA with p-value < 0.05), a Wilcoxon signed-rank test, a test for paired differences in non-normally distributed data, was performed to identify stimulation conditions that were significantly different from random stimulation.

The Wilcoxon test was also applied to determine the stimulation conditions that showed a significant improvement in working memory performance due to the intervention. For these tests, mean values of each session were used to avoid over-fitting the data if counting each of the 100 trials per session individually. On the other hand, using only the means could have led to a potentially underestimated effect size. For comparing stimulation conditions, the mean values were subtracted from each other (the before value was subtracted from the after value).

The strength of the effect was determined by calculating Hedge's g with the following formula:

$$g = \frac{x_1 - x_2}{\sqrt{\dfrac{(n_1 - 1) \cdot sd_1^2 - (n_2 - 1) \cdot sd_2^2}{(n_1 + n_2) - 2}}} \cdot \frac{n - 3}{n - 2,25} \cdot \sqrt{\frac{n - 2}{n}} \tag{2.1}$$

x = means of samples
n = sample size
sd = standard deviation of samples

Hedge's g is better suited than Cohen's d when dealing with sample sizes smaller than 20. However, both can over-estimate samples smaller than 50. This can be counteracted by using a correction factor, which is included above [Ellis, 2010; Hedges, 1981]. It reduces the effect size of smaller samples by a small fraction.

The values of effect size can be interpreted in the following way [J. Cohen, 1988]:

- Values around 0.2 represent a small effect size.

- Values around 0.5 signify a medium effect size.

- Values around and above 0.8 describe a large effect size.

2.5 Own Contributions

The study was designed in collaboration with Dr. Pedro Gordon (postdoc) and Dr. Christoph Zrenner (postdoc). The development of the applied method of EEG-triggered stimulation was done by Pedro Gordon and Christoph Zrenner. The selection and configuration of the working memory task were done by me. The experiments were conducted by me in collaboration with Pedro Gordon, Dragana Galevska (research assistant), and Anna Kempf (research assistant). The statistical analysis was performed independently by me, except for the analysis of the accuracy of the phase-detection algorithm, which was conducted by Pedro Gordon.

3 Results

3.1 Accuracy of Phase Detection

One key point for the reliability of our results is the preciseness of the stimulation time and, therefore, the accuracy of the phase detection algorithm. This accuracy is visualized in Figure 3.1, which includes mean value and SD with $0°$ corresponding to the positive peak and $180°$ to the negative peak (trough). The mean positive peak, as determined by the algorithm, was at $-5° \pm 63°$, and for the negative peak, it was at $173°$ $\pm 42°$. It shows the distributions of the post-hoc identified phase of the theta oscillation at the time when the algorithm predicted the phase and would trigger stimulation to either hit the positive or the negative peak of the theta oscillation.
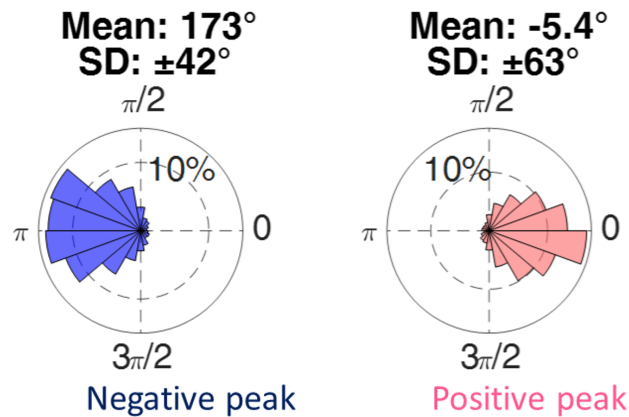
Figure 3.1: Illustration of the accuracy of our phase estimation algorithm. With 0° being the top of the positive peak and 180° or respectively π being the top of the negative peak. The inner ring indicates 10% of all phase estimations.
[Image source: Gordon, Dörre, et al., 2021]

3.2 Sternberg Task

For generating Figures 3.2 and 3.3, and for analysis of the reaction time, only correct responses were included. Considering that the goal is a working memory improvement, it is more relevant for subjects to be faster when giving correct responses rather than having a reaction time improvement for incorrect responses. In addition, an analysis with the values of reaction times from all responses is included as well.

As indicated in Table 3.1, the mean reaction time decreased after stimulation both for the stimulation at the negative peak (by $0.06s$) and for the stimulation at the positive peak (by $0.01s$). For the random stimulation, the mean reaction time increased by $0.01s$. The mean accuracy remained almost consistent for the stimulation at the negative and the positive peak. For the random stimulation, the accuracy increased by 1% after the intervention. These results are illustrated in Figure 3.2 and 3.3.

The results of a linear mixed models analysis were checked by an ANOVA for significant interactions. As shown in Table 3.2, the reaction times for correct and for all responses were significantly different between conditions, time states, and the interaction of

Table 3.1: Mean and SD of reaction times (correct responses only) and accuracies at each condition and time state.

	Time state (relative to intervention)	Conditions mean and SD		
		Negative peak	Positive peak	Random
Reaction time	Before	1.08 ± 0.14	1.06 ± 0.18	1.07 ± 0.15
(in seconds)	After	1.02 ± 0.12	1.05 ± 0.17	1.08 ± 0.18
Accuracy	Before	76.6 ± 7	76.7 ± 7	75.4 ± 6
(in percent)	After	76.6 ± 6	76.2 ± 6	76.8 ± 7

Table 3.2: P-values of the performed ANOVA on the linear mixed models of the reaction time and the accuracy of responses. P-values < 0.05 are marked by *

	ANOVA on linear mixed effects		
	Conditions	Time states	Conditions/states
Reaction time - only correct responses	$p = 0.0003$*	$p = 0.0001$*	$p = 0.002$*
Reaction time - all responses	$p = 0.002$*	$p = 0.0000$*	$p = 0.003$*
Accuracy	$p = 0.92$	$p = 1$	$p = 0.64$

conditions and time states, with a p-value < 0.05. An analysis of the combined effects of stimulation conditions and time states also showed that reaction times before and after stimulation were significantly different.

The accuracy of responses did not vary significantly in every aspect.

3.2.1 Reaction Time

After revealing non-normally distributed data by a one-sample Kolmogorov-Smirnov test ($p < 0.001$), a dependent Wilcoxon signed-rank test was used to further analyze any data that were significant in the above-mentioned ANOVA. We analyzed which of the stimulation conditions was significantly different ($p < 0.05$) from the other stimulation conditions, respectively, with the results presented in Table 3.3. For the

Table 3.3: P-values of a dependent Wilcoxon signed rank test comparing the means of the change in reaction time (post- vs. pre-intervention) of each stimulation condition to another stimulation condition. The significant p-values (< 0.05) are marked by *

	Wilcoxon on conditions		
	Negative peak vs. random	Positive peak vs. random	Negative vs. positive peak
Reaction time - only correct responses	$p = 0.02^*$	$p = 0.26$	$p = 0.44$
Reaction time - all responses	$p = 0.16$	$p = 0.80$	$p = 0.33$

Table 3.4: P-values of a dependent Wilcoxon signed rank test comparing the means of the reaction time of each session's responses before versus after stimulation, respectively. The significant p-values (< 0.05) are marked by *

	Wilcoxon on time state		
	Negative peak	Positive peak	Random
Reaction time - only correct responses	$p = 0.01^*$	$p = 0.68$	$p = 0.50$
Reaction time - all responses	$p = 0.02^*$	$p = 0.80$	$p = 0.61$

negative peak condition compared to random stimulation, the analysis demonstrates a significant difference in reaction times for correct responses ($p = 0.02$). The positive peak stimulation was not significantly different from the random stimulation ($p = 0.26$). Another analysis compared differences in reaction times before intervention with the reaction times after for each stimulation condition separately, with the results shown in Table 3.4. Only stimulation at the negative peak of the theta phase resulted in significant differences for before versus after stimulation with this analysis.

Figure 3.2 shows reaction times of the Sternberg task in a grouped whisker plot. The center bar indicates the median, and the edges of the box indicate the 25th and 75th percentiles, respectively. The whiskers contain values of 1.5 of the interquartile range. Outliers outside the range of the whiskers are marked by +. Green diamonds

symbolize mean values. In the graphic the trend of the reduction of reaction times for the negative peak condition is visible and highlighted by a connecting line in blue. A modest reduction of reaction times can be distinguished for the positive peak condition, which is visualized by a red line. Concerning the random condition, the trend is featured by a grey line and demonstrates a modest tendency toward an increase in reaction times.

The strength of effect was calculated using Equation 2.1, with the result of a medium effect strength with $g = 0.497$ (see Section 2.4.3).

3.2.2 Accuracy

The results of subjects' accuracy in the Sternberg task are visualized in Figure 3.3. As mentioned above, there were no significant changes in the accuracy of subjects' responses. However, the results can also be used to determine if the level of difficulty of the working memory task was sufficient, as mentioned earlier. For all sessions, the accuracy was well above chance level but also low enough to have the potential for improvement, thus avoiding a ceiling or floor effect. The lowest accuracy achieved was at 60%, and the highest value was 90%, with the median values distant from extreme values.
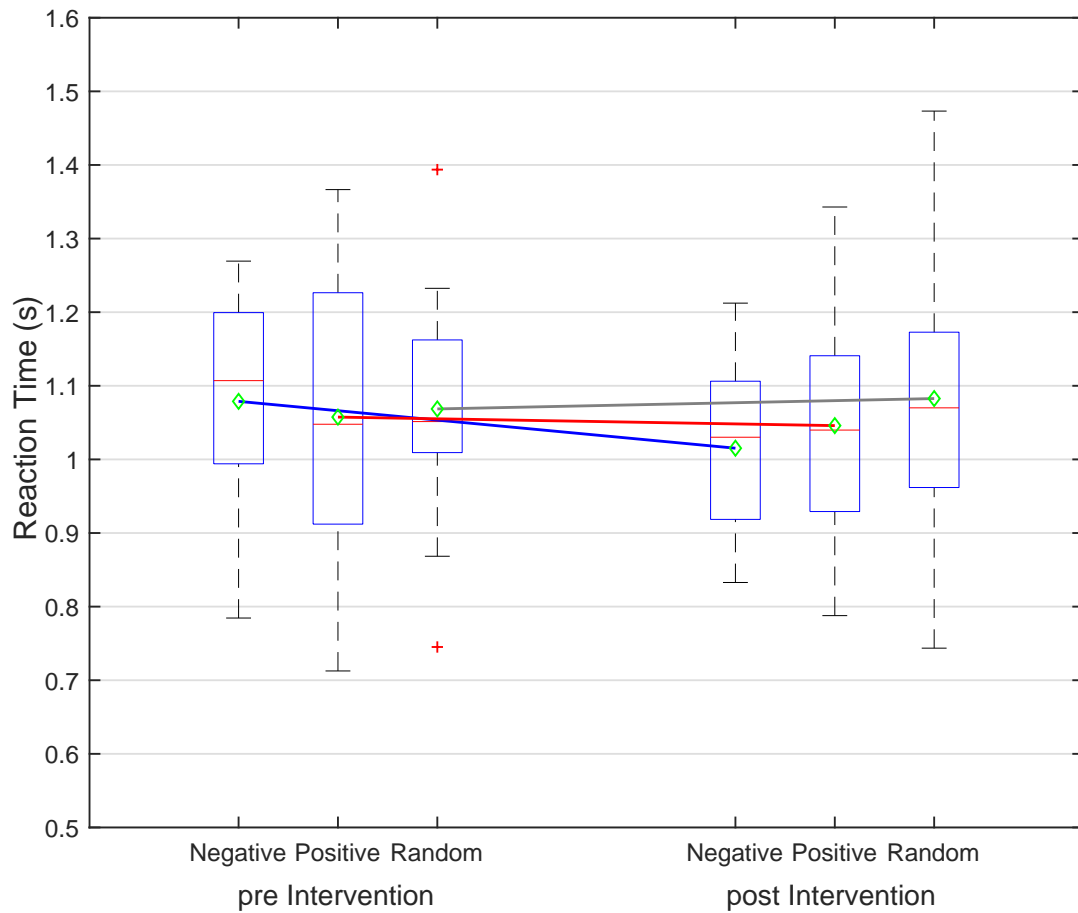
Figure 3.2: Distribution of subjects' reaction times of correctly answered trials in a grouped whisker plot. The data are grouped depending on measurements collected before or after intervention and split into the different stimulation conditions, i.e., negative peak, positive peak, or random stimulation with connecting lines to visualize the respective trends in blue, red, and grey.
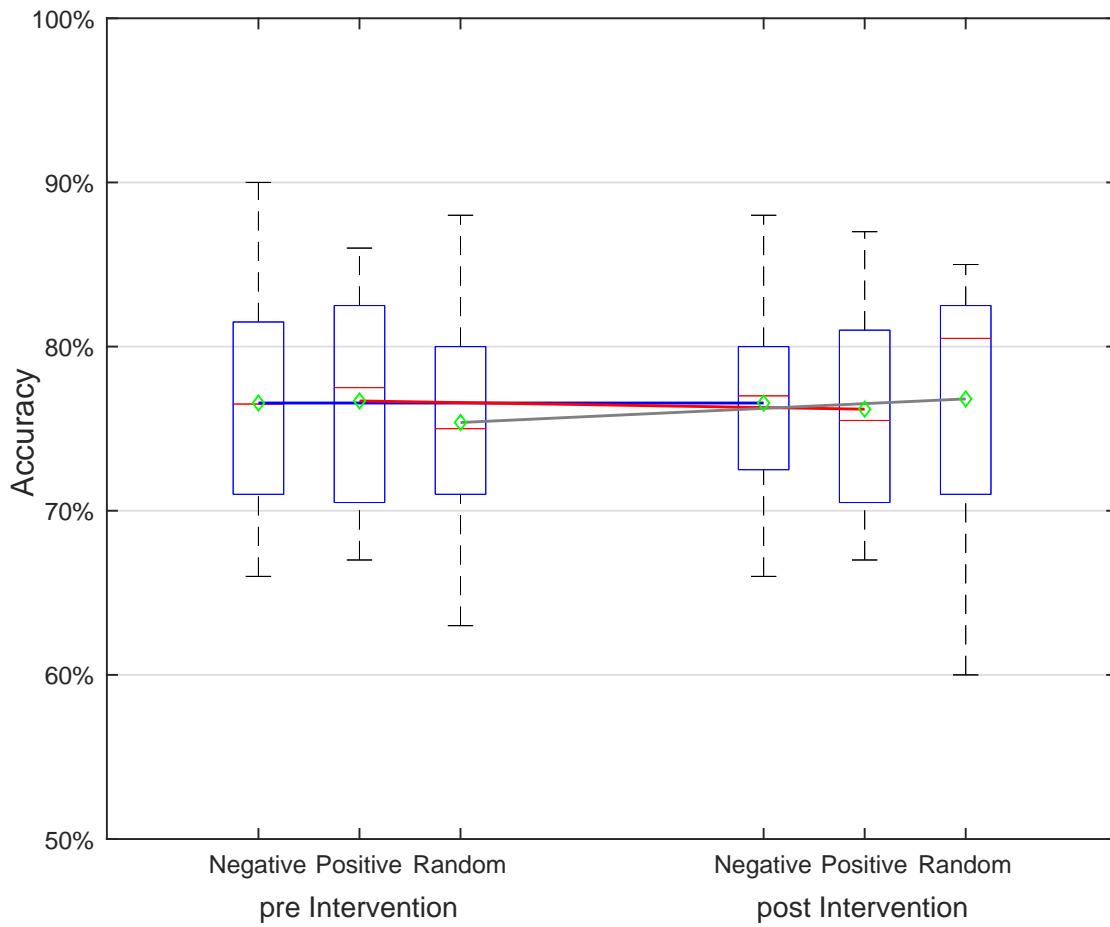
Figure 3.3: Display of the accuracy of subject's responses in percent in a grouped whisker plot. The data are grouped depending on measurements collected before or after intervention and split into the different stimulation conditions, i.e., negative peak, positive peak, or random stimulation with connecting lines to visualize the respective trends in blue, red, and grey.

4 Discussion

4.1 Related Work

This chapter starts with an evaluation of our results in the context of current literature, followed by a discussion of the stimulation and task aspects of the experiment. The chapter ends with a conclusion and a perspective for the future.

The results presented in the previous chapter strongly suggest that synchronizing TMS with the negative peak of the ongoing FM-theta oscillation has a significant impact on repetitive stimulation, resulting in different behavioral effects as a consequence of a repetitive TMS protocol. Stimulation at the trough phase of theta resulted in shorter reaction times in the Sternberg task compared to a random stimulation, with a medium effect size of 0.497 (for classification of ranges, see Section 2.4.3). In comparison, non-phase-triggered non-invasive brain stimulation of the dlPFC shows mixed results in improving working memory function, with either a slight improvement or none at all [Berryhill et al., 2012; Boggio et al., 2006; Guse et al., 2013]. Of note, the latter method is currently applied in the therapy of depression. By combining existing non-invasive brain stimulation studies into a meta-analysis, Brunoni et al. could show an improvement in reaction times with a small effect size of 0.22 [Brunoni et al., 2014]. The studies included in this meta-analysis had a similar number of participants compared to our study, making a reliable comparison possible. The effect size of this meta-analysis

is noticeably smaller than the effect size obtained by our method. This could either be due to the different stimulation target, the phase-dependent stimulation approach we used, or both.

4.2 Stimulation Aspects

When aiming to stimulate a specific phase, it is crucial to know how precisely the phase is actually targeted. The accuracy of our phase detection algorithm is comparable to similar algorithms published before [Siegle et al., 2014; Zrenner, Desideri, et al., 2018] despite facing challenges such as working with an inconsistent oscillation and a low signal-to-noise ratio. For example, Zrenner et al. achieved an accuracy of $0°$ $\pm53°$ (positive peak) and $181°\pm55°$ (negative peak) for phase-dependent stimulation of sensorimotor μ-rhythm. Unfortunately, there are very little data available on the subject because of the as of yet limited amount of studies performing an EEG-phase-locked stimulation in the first place and the even more limited amount of these studies reporting the accuracy of their phase estimation.

One limitation of an EEG stimulation that is phase-locked to the theta rhythm compared to the sensorimotor μ-rhythm is that there are no single trial markers of excitability. In contrast, in the motor system, the amplitude of the muscle contraction in each trial can be measured as motor evoked potential.

Another limitation of working with the theta rhythm is that an inconsistent oscillation like the FM-theta complicates a phase estimation considerably. Phase predictions calculated from more extended periods of the oscillations are more likely to be accurate compared to estimations calculated from a shorter period as there are more data to extrapolate from. However, in the case of FM-theta, a more prolonged period of the oscillation is more likely to contain phase resets, which occur approximately at least

every two seconds [Kahana et al., 1999]. Consequently, the algorithm must verify if the current signal corresponds to a stable oscillation and that the utilized period does not contain phase resets. This was managed by incorporating specific limitations into the algorithm.

Additionally, the lower signal-to-noise ratio of the FM-theta leads to a higher sensitivity of the extracted signal to be distorted by other oscillations. This results in a decreased accuracy of the phase detection algorithm [Zrenner, Galevska, et al., 2020]. By using individual filters for extracting the oscillation, we argue that a clearer signal could be attained compared to standardized filters [Gordon, Dörre, et al., 2021]. However, it is unclear how close the extracted signal is to the actual endogenously occurring signal, raising the possibility that the signal is still tainted slightly by other oscillations. This might result in lower accuracy of the phase estimation than suggested by our analysis.

As mentioned in the first chapter, our stimulation method considers endogenous mechanisms of the brain, such as phase-amplitude coupling. This mechanism seems essential for learning processes by inducing synaptic plasticity and being utilized for storing information currently held in working memory. Thus, on the one hand, imitating this mechanism should foster synaptic plasticity to achieve effects that outlast the stimulation itself. This is an essential issue because the stimulation in our experiment was temporally separate from the working memory task. Therefore, any observed changes in brain activity due to stimulation would have to persist for a certain period after the intervention. Besides, any intervention used as a treatment in medicine should ideally induce long-lasting effects to make the treatment only necessary for a couple of sessions. Effects on the motor cortical excitability could already be demonstrated by Zrenner et al. after applying high-frequency bursts of stimulation phase-locked to the sensorimotor μ-alpha-oscillation [Zrenner, Desideri, et al., 2018].

On the other hand, the question is whether by imitating these mechanisms, the brain is being trained in some way to use its activity more effectively in working memory activity. However, it is uncertain whether this stimulation might train the brain to synchronize its oscillations more effectively.

4.3 Task Aspects

Two possible factors influencing the results of the working memory task are a learning effect and a higher degree of exhaustion during the trials after the intervention. A learning effect for the task could make a working memory improvement seem more significant than it actually is by improving only the post-intervention parameters. It may also result in differences between sessions if they are not adequately separated in time. However, the individual sessions for a subject were always at least one week apart, thus making a learning effect across sessions quite unlikely. Furthermore, a learning effect across sessions would affect both pre- and post-intervention parameters, thus not influencing the difference between the two parameters, i.e., memory improvement. Moreover, a learning effect within one session would affect each of the sessions equally, including the random session, making it harder to spot differences between the different conditions. Therefore, a possible learning effect would only result in a less significant difference between a phase-dependent and a random stimulation, leading to a smaller effect size. Additionally, with each session of the experiment lasting about four hours, including preparation time, it is also possible for participants to be increasingly tired and thus be less attentive for the final step of each session, the working memory task. This could decrease working memory performance and negate the possible learning effect, making it more challenging to determine memory improvements. In conclusion,

in a fictional scenario where learning effects and tiredness do not exist, we expect to detect a more considerable improvement in working memory compared to what we reported here.

While the analysis could demonstrate significant differences between the stimulation conditions for reaction times in the Sternberg task, it is worth mentioning that the results for changes in accuracy in the task show no different effects at all. Comparing the accuracies of the different stimulation conditions, they are noticeably similar. Since the accuracies are almost identical, it is not to be expected to attain significant results, even increasing the sample size by a considerable amount.

Apart from this, the suitability of the Sternberg task for our experiment needs to be discussed. When initially selecting the working memory task, the planned stimulation target of the experiment was different from what it ended up being. The intended primary stimulation target was the left dlPFC as it is the main region currently targeted for stimulation to achieve working memory improvement and treatment of depression. This is due to its contribution to working memory functions and an association between hypoactivity in this brain region and depression [Barbey et al., 2013; George, Ketter, et al., 1994]. For this reason, our original research to find a suitable working memory task was based on working memory improvement through non-invasive brain stimulation of the dlPFC [Brunoni et al., 2014; Dedoncker et al., 2016]. Looking for well-established working memory tasks in this niche, we found that studies using either the n-back task or the Sternberg task showed the most promising working memory improvement effects.

One difference between the tests that was crucial to us is that in the n-back task, trials are not independent units but are connected, while in the Sternberg task, each trial is separate from the rest. The Sternberg task has the additional advantage of temporal separation of stimulus, retention, and query. This is important because it

creates the possibility to also correlate neurophysiological and behavioral outcomes, besides analyzing working memory improvement for a further analysis not included in this thesis.

However, as mentioned above, we selected the dmPFC as the stimulation target instead of the dlPFC. For our method of phase-dependent stimulation, it is essential to acquire a high signal-to-noise-ratio oscillation signal. Therefore, it is essential to target a specific oscillation instead of an anatomical target to improve working memory. Accordingly, the selection of the dmPFC as stimulation target was decided to achieve a reliable phase estimation for the phase-specific stimulation because testing of the spatial filter resulted in a signal-to-noise ratio of the theta oscillation in favor of the dmPFC.

Nevertheless, the Sternberg task as a classic verbal working memory retention task is also well suited to assess changes in medial PFC activity or rather FM-theta activity as this theta oscillation seems to be responsible for working memory retention [Jensen and Tesche, 2002]. Besides, the primary conditions of the experiment did not change with the objective of achieving working memory improvement remaining unaffected, and only the method through which it would be reached changed slightly. Moreover, the considerations above are supported by the fact that the task could detect a significant working memory improvement in our experiment.

While the dlPFC is more widely associated with working memory than the dmPFC, there is another possible explanation for the more considerable improvement in reaction times we obtained, compared to other recent studies mentioned before [Funahashi et al., 1994]. One cognitive function associated with the dmPFC is decision-making under uncertainty [Nachev et al., 2005; Ullsperger et al., 2001]. As our experiment resulted only in a shorter reaction time without improvement of accuracy, it is possible that the stimulation did not actually improve working memory's accuracy but instead improved decision-making for trials where participants were unsure of the correct

response. If, however, the results were achieved solely by improving the decision-making function rather than the working memory function, this would influence both correct and incorrect responses equally. This is unlikely because we analyzed both the reaction times with only the correct responses included and all reaction times separately. Here, only the analysis with just the correct responses yielded significant results.

Since the dmPFC is more often associated with emotional control, cognitive control, and decision making than with working memory, it could be argued that a different objective could be more suitable for stimulation of the dmPFC [E. K. Miller et al., 2001; M. L. Phillips et al., 2008; Venkatraman et al., 2009]. However, this would make the method more difficult to compare to recent studies and, therefore, more challenging to apply to treatments of non-healthy subjects. On the one hand, the above-mentioned cognitive functions could be good markers for treatment for depression, for example, on the other hand, they are not commonly used to evaluate the efficacy of TMS treatment. As new treatments need to be evaluated compared to existing treatments, this would make the admission of the method more challenging.

4.4 Conclusion and Future Perspective

To conclude this chapter, our algorithm detected the ongoing phase of theta with an accuracy comparable to other phase detection algorithms, despite facing difficulties targeting the theta oscillation. In addition, possible influencing factors such as a learning effect of the task or an exhaustion effect at the end of sessions were adequately controlled for in the study design. Also, they would lead to a lower chance of achieving significant results instead of making them seem more significant than they actually are. Besides, the Sternberg task was sufficient to demonstrate the stimulation's behavioral changes in working memory performance.

Nevertheless, it might be interesting to conduct an experiment in which our method of stimulation to the dmPFC is evaluated by the performance in a decision-making task instead of a working memory task because of its relevance for dmPFC function as mentioned previously.

Besides this, there are different possibilities to improve the aspect of the accuracy of the phase-dependent stimulation. One possibility would be to create a better environment for the prediction with a more distinct and consistent theta oscillation by influencing the brain's current state. Moreover, better accuracy for the stimulation could also be achieved by inducing a more pronounced signal for the algorithm, meaning an oscillation with higher amplitudes and thereby achieving an improved signal-to-noise ratio [Zrenner, Galevska, et al., 2020]. For the FM-theta oscillation specifically, this could be achieved through tasks of sustained internally-directed cognition attention [Hsieh, Ekstrom, et al., 2011; Raghavachari et al., 2001; Tsujimoto et al., 2010]. Therefore, a retention or continuous visuospatial task without external stimuli could be employed during the stimulation period to create an improved signal-to-noise ratio, possibly resulting in a higher accuracy [Kahana et al., 1999].

To possibly achieve a greater effect with the stimulation, one could try to target a different phase of theta aside from peak or trough. This aspect could be analyzed in a follow-up experiment.

Additionally, as the conducted experiment was planned as a pilot study for testing a new method on a smaller scale on healthy subjects, an ensuing study on a larger scale with participants with a psychiatric disorder associated with working memory deficits should be conducted. This has the potential to lead to the establishment of an improved protocol for TMS treatments.

5 Summary

The experimental results presented in this thesis indicate that theta phase-specific stimulation of the dmPFC leads to an improved reaction time in the Sternberg working memory task when targeting the trough of the FM-theta oscillation.

To achieve a phase-dependent stimulation we use real-time phase estimation by creating spatial filters for EEG data to isolate the ongoing oscillation of the dmPFC. The isolated oscillation is filtered and analyzed in multiple steps to attain an instantaneous phase estimation. With this estimation of the theta phase, TMS pulses can be triggered depending on the current phase. Participants perform a Sternberg working memory task before and after the intervention with this phase-dependent stimulation. Each session is randomized regarding the targeted phase that was stimulated, which is either a random phase, the peak, or the trough of the FM-theta oscillation.

Employing an ANOVA, this work shows that significant differences exist between the three stimulation conditions in terms of the effect on the working memory task performance. A Wilcoxon test confirms these differences for the stimulation at the trough of the theta rhythm compared to stimulation at a random time point in the theta phase. For this, the analysis shows shortened response times in the Sternberg task after trough stimulation with an effect size of 0.497. However, the proportion of correct responses does not change significantly due to the different simulation conditions.

Comparing our results to current literature, the effect size of the reaction time improvement in the working memory task is greater than the effect sizes of experiments that used a non-phase-triggered stimulation. In addition, it is shown that the accuracy of the phase-dependent stimulation corresponds to the current standard.

Moreover, various factors potentially influencing working memory performance aside from the TMS are discussed in this work with the conclusion that they would instead lead to a possible underestimation rather than an overestimation of our results' significance. Furthermore, the Sternberg task proves to be sufficient in demonstrating improved working memory performance as an effect of the stimulation. Our results on healthy subjects indicate that our designed method could help refine current TMS therapy protocols and, thereby, improve response rates of TMS therapy.

6 Zusammenfassung

Diese Arbeit zeigt, dass die phasenspezifische transkranielle Magnetstimulation (TMS) in Abhängigkeit des Thetarhythmus des dmPFC zu einer signifikanten Verbesserung der Reaktionszeit bei einer Arbeitsgedächtnisaufgabe führt.

Die phasenspezifische Stimulation basiert auf einer Echtzeitprognose der aktuellen Phase des Thetarhythmus. Hierzu wird ein Filter erstellt, der die EEG-Daten nach einer räumlichen Quelle filtert, um die derzeitige Oszillation des dmPFC zu isolieren. Die extrahierte Oszillation wird in mehreren Schritten analysiert, um eine Echtzeit-Phasenschätzung zu erhalten. Mit dieser Prognose der Theta-Phase werden TMS Pulse in Abhängigkeit von der aktuellen Phase ausgelöst. Die Teilnehmer führen vor und nach der Intervention mit dieser phasenabhängigen Stimulation jeweils Sternberg-Aufgaben zur Testung des Arbeitsgedächtnisses durch. Die einzelnen Sitzungen werden hinsichtlich der ausgewählten Phase, die stimuliert werden soll, randomisiert, wobei die Stimulation entweder am Höhepunkt, am Tiefpunkt oder an einem zufälligen Zeitpunkt in der Phase der frontalen Thetaschwingung stattfindet.

Diese Arbeit zeigt mittels einer ANOVA, dass signifikante Unterschiede in der Reaktionszeit zwischen den drei Stimulationsbedingungen in der Sternberg-Aufgabe bestehen. Ein Wilcoxon-Test bestätigt diese Unterschiede für die Stimulation des Tiefpunkts des Thetarhythmus im Vergleich zu einer Stimulation an einem zufälligen Zeitpunkt der Thetaphase. Hier zeigt die Analyse kürzere Reaktionszeiten in der Sternberg-Aufgabe

nach der Stimulation des Tiefpunktes mit einer Effektgröße von $0,497$. Der Anteil der korrekten Antworten ändert sich dabei allerdings nicht signifikant in Abhängigkeit der unterschiedlichen Simulationsbedingungen.

Vergleicht man unsere Ergebnisse mit der aktuellen Literatur, so ist die Effektgröße der Reaktionszeitverbesserung in der Arbeitsgedächtnisaufgabe größer als die Effektgrößen von Experimenten, die eine nicht-phasenspizifische Stimulation durchführten. Zusätzlich ist die Genauigkeit der Phasenbestimmung vergleichbar mit ähnlichen Experimenten.

Zusätzlich wird in dieser Arbeit aufgezeigt, dass mögliche Einflussfaktoren auf die Arbeitsgedächtnisleistung, abgesehen von der TMS, eher dazu führen würden, dass die Signifikanz unserer Ergebnisse unter- anstatt überschätzt wird. Darüber hinaus erwies sich die Sternberg-Aufgabe als geeignet, um eine verbesserte Arbeitsgedächtnisleistung als Effekt der Stimulation zu demonstrieren. Unsere Ergebnisse an gesunden Probanden deuten darauf hin, dass die von uns entwickelte Methode nützlich sein könnte, um die derzeitigen TMS-Therapieprotokolle zu optimieren und dadurch die Ansprechraten und somit auch die Wirksamkeit der TMS-Therapie zu verbessern.

7 References

Arieli, A., A. Sterkin, A. Grinvald, A. Aertsen (1996). "Dynamics of Ongoing Activity: Explanation of the Large Variability in Evoked Cortical Responses." In: *Science* 273.5283, pp. 1868–1871. DOI: `10.1126/science.273.5283.1868` (cit. on p. 12).

Avery, D. H., K. E. Isenberg, S. M. Sampson, P. G. Janicak, S. H. Lisanby, D. F. Maixner, et al. (2008). "Transcranial magnetic stimulation in the acute treatment of major depressive disorder: clinical response in an open-label extension trial." In: *Journal of Clinical Psychiatry* 69.3, pp. 441–451 (cit. on p. 11).

Axmacher, N., F. Mormann, G. Fernández, C. E. Elger, J. Fell (2006). "Memory formation by neuronal synchronization." In: *Brain Research Reviews* 52.1, pp. 170–182. DOI: `10.1016/j.brainresrev.2006.01.007` (cit. on p. 20).

Baddeley, A. (2000). "The episodic buffer: a new component of working memory?" In: *Trends in Cognitive Sciences* 4.11, pp. 417–423. DOI: `10.1016/S1364-6613(00)01538-2` (cit. on p. 13).

Barbey, A. K., M. Koenigs, J. Grafman (2013). "Dorsolateral prefrontal contributions to human working memory." In: *Cortex* 49.5, pp. 1195–1205. ISSN: 0010-9452. DOI: `10.1016/j.cortex.2012.05.022` (cit. on p. 59).

Barch, D. M., Y. I. Sheline, J. G. Csernansky, A. Z. Snyder (2003). "Working memory and prefrontal cortex dysfunction: specificity to schizophrenia compared with major depression." In: *Biological Psychiatry* 53.5, pp. 376–384. DOI: `10.1016/S0006-3223(02)01674-8` (cit. on p. 15).

Bauer, R. H., J. M. Fuster (1976). "Delayed-matching and delayed-response deficit from cooling dorsolateral prefrontal cortex in monkeys." In: *Journal of Comparative and Physiological Psychology* 90.3, pp. 293–302. DOI: `10.1037/h0087996` (cit. on p. 14).

Benchenane, K., A. Peyrache, M. Khamassi, P. L. Tierney, Y. Gioanni, F. P. Battaglia, S. I. Wiener (2010). "Coherent Theta Oscillations and Reorganization of Spike Timing in the Hippocampal- Prefrontal Network upon Learning." In: *Neuron* 66.6, pp. 921–936. DOI: `10.1016/j.neuron.2010.05.013` (cit. on p. 18).

Berger, B., B. Griesmayr, T. Minarik, A. L. Biel, D. Pinal, A. Sterr, P. Sauseng (2019). "Dynamic regulation of interregional cortical communication by slow brain oscillations during working memory." In: *Nature Communications* 10.1. DOI: `10.1038/s41467-019-12057-0` (cit. on p. 27).

Bergmann, T. O., A. Karabanov, G. Hartwigsen, A. Thielscher, H. R. Siebner (2016). "Combining non-invasive transcranial brain stimulation with neuroimaging and electrophysiology: Current approaches and future perspectives." In: *NeuroImage* 140, pp. 4–19. DOI: `10.1016/j.neuroimage.2016.02.012` (cit. on p. 26).

Berryhill, M. E., K. T. Jones (2012). "tDCS selectively improves working memory in older adults with more education." In: *Neuroscience Letters* 521.2, pp. 148–151. DOI: `10.1016/j.neulet.2012.05.074` (cit. on p. 55).

Bliss, T. V. P., G. L. Collingridge (1993). "A synaptic model of memory: long-term potentiation in the hippocampus." In: *Nature* 361.6407, pp. 31–39. DOI: `10.1038/361031a0` (cit. on p. 20).

Bliss, T. V. P., T. Lomo (1973). "Long-lasting potentiation of synaptic transmission in the dentate area of the anaesthestized rabbit following stimulation of the perforant path." In: *J. Physiol. 232 : 33 1-56* (cit. on p. 20).

Blumberger, D. M., F. Vila-Rodriguez, K. E. Thorpe, K. Feffer, Y. Noda, P. Giacobbe, et al. (2018). "Effectiveness of theta burst versus high-frequency repetitive transcranial magnetic stimulation in patients with depression (THREE-D): a randomised non-inferiority trial." In: *The Lancet* 391.10131, pp. 1683–1692. DOI: `10.1016/S0140-6736(18)30295-2` (cit. on p. 25).

Boggio, P. S., R. Ferrucci, S. P. Rigonatti, P. Covre, M. Nitsche, A. Pascual-Leone, F. Fregni (2006). "Effects of transcranial direct current stimulation on working memory in patients with Parkinson's disease." In: *Journal of the Neurological Sciences* 249.1, pp. 31–38. DOI: `10.1016/j.jns.2006.05.062` (cit. on p. 55).

Brunoni, A. R., M.-A. Vanderhasselt (2014). "Working memory improvement with non-invasive brain stimulation of the dorsolateral prefrontal cortex: A systematic review and meta-analysis." In: *Brain and Cognition* 86, pp. 1–9. DOI: `10.1016/j.bandc.2014.01.008` (cit. on pp. 55, 59).

Buzsáki, G., A. Draguhn (2004). "Neuronal Oscillations in Cortical Networks." In: *Science* 304.5679, pp. 1926–1929. DOI: `10.1126/science.1099745` (cit. on p. 18).

Cajal, S. R. y. (1894). "The Croonian lecture.—La fine structure des centres nerveux." In: *Proceedings of the Royal Society of London* 55.331-335, pp. 444–468. DOI: `10.1098/rspl.1894.0063` (cit. on p. 20).

Carlén, M. (2017). "What constitutes the prefrontal cortex?" In: *Science* 358.6362, pp. 478–482. DOI: `10.1126/science.aan8868` (cit. on pp. 14, 15).

Cavanagh, J. F., M. X. Cohen, J. J. B. Allen (2009). "Prelude to and Resolution of an Error: EEG Phase Synchrony Reveals Cognitive Control Dynamics during Action Monitoring." In: *Journal of Neuroscience* 29.1, pp. 98–105. DOI: `10.1523/JNEUROSCI.4137-08.2009` (cit. on p. 19).

Cavanagh, J. F., M. J. Frank (2014). "Frontal theta as a mechanism for cognitive control." In: *Trends in Cognitive Sciences* 18.8, pp. 414–421. DOI: `10.1016/j.tics.2014.04.012` (cit. on p. 19).

Cohen, J. (1988). *Statistical Power Analysis for the Behavioral Sciences*. Routledge. DOI: `10.4324/9780203771587` (cit. on p. 45).

Cole, E. J., A. L. Phillips, B. S. Bentzley, K. H. Stimpson, R. Nejad, F. Barmak, et al. (2022). "Stanford Neuromodulation Therapy (SNT): A double-blind randomized controlled trial." In: *American Journal of Psychiatry* 179.2, pp. 132–141. DOI: `10.1176/appi.ajp.2021.20101429` (cit. on p. 12).

Cole, E. J., K. H. Stimpson, B. S. Bentzley, M. Gulser, K. Cherian, C. Tischler, et al. (2020). "Stanford accelerated intelligent neuromodulation therapy for treatment-resistant depression." In: *American Journal of Psychiatry* 177.8, pp. 716–726. DOI: `10.1176/appi.ajp.2019.19070720` (cit. on p. 12).

Colgin, L. L. (2011). "Oscillations and hippocampal–prefrontal synchrony." In: *Current Opinion in Neurobiology* 21.3, pp. 467–474. DOI: `10.1016/j.conb.2011.04.006` (cit. on p. 19).

Costafreda, S. G., C. H. Fu, L. Lee, B. Everitt, M. J. Brammer, A. S. David (2006). "A systematic review and quantitative appraisal of fMRI studies of verbal fluency: Role of the left inferior frontal gyrus." In: *Human Brain Mapping* 27.10, pp. 799–810. DOI: `10.1002/hbm.20221` (cit. on p. 16).

Courtney, S. M., L. G. Ungerleider, K. Keil, J. V. Haxby (1997). "Transient and sustained activity in a distributed neural system for human working memory." In: *Nature* 386.6625, pp. 608–611. DOI: `10.1038/386608a0` (cit. on p. 14).

Cowan, N. (1998). *Attention and memory: An integrated framework*. Oxford University Press (cit. on p. 14).

D'Esposito, M., B. R. Postle (2015). "The Cognitive Neuroscience of Working Memory." In: *Annual Review of Psychology* 66.1, pp. 115–142. DOI: `10.1146/annurev-psych-010814-015031` (cit. on p. 14).

Daskalakis, Z. J., A. J. Levinson, P. B. Fitzgerald (2008). "Repetitive Transcranial Magnetic Stimulation for Major Depressive Disorder: A Review." In: *The Canadian Journal of Psychiatry* 53.9, pp. 555–566. DOI: `10.1177/070674370805300902` (cit. on p. 12).

Dedoncker, J., A. R. Brunoni, C. Baeken, M.-A. Vanderhasselt (2016). "A Systematic Review and Meta-Analysis of the Effects of Transcranial Direct Current Stimulation (tDCS) Over the Dorsolateral Prefrontal Cortex in Healthy and Neuropsychiatric Samples: Influence of Stimulation Parameters." In: *Brain Stimulation* 9.4, pp. 501–517. DOI: `10.1016/j.brs.2016.04.006` (cit. on pp. 43, 59).

Dehn, M. J. (2015). *Essentials of Working Memory Assessment and Intervention*. Ed. by A. S. Kaufman, N. L. Kaufman, M. J. Dehn. John Wiley and Sons Inc. 320 pp. ISBN: 1118638131 (cit. on p. 15).

Deutsche Gesellschaft Für Psychiatrie, Psychotherapie Und Nervenheilkunde (DGPPN), Ärztliches Zentrum Für Qualität In Der Medizin (ÄZQ) (2017). *S3-Leitlinie/Nationale VersorgungsLeitlinie Unipolare Depression - Langfassung, 2. Auflage Version 5*. de. Deutsche Gesellschaft für Psychiatrie, Psychotherapie und Nervenheilkunde (DGPPN); Bundesärztekammer (BÄK); Kassenärztliche Bundesvereinigung (KBV); Arbeitsgemeinschaft der Wissenschaftlichen Medizinischen Fachgesellschaften (AWMF). DOI: `10.6101/AZQ/000364` (cit. on p. 11).

Diamond, A. (2013). "Executive Functions." In: *Annual Review of Psychology* 64.1, pp. 135–168. DOI: `10.1146/annurev-psych-113011-143750` (cit. on p. 13).

Downar, J., Z. J. Daskalakis (2013). "New Targets for rTMS in Depression: A Review of Convergent Evidence." In: *Brain Stimulation* 6.3, pp. 231–240. DOI: `10.1016/j.brs.2012.08.006` (cit. on p. 12).

Ellis, P. D. (2010). *The essential guide to effect sizes: Statistical power, meta-analysis, and the interpretation of research results*. Cambridge university press. ISBN: 9781139488150 (cit. on p. 45).

Faul, F., E. Erdfelder, A. Buchner, A.-G. Lang (2009). "Statistical power analyses using G* Power 3.1: Tests for correlation and regression analyses." In: *Behavior research methods* 41.4, pp. 1149–1160. DOI: `10.3758/BRM.41.4.1149` (cit. on p. 43).

Faul, F., E. Erdfelder, A.-G. Lang, A. Buchner (2007). "G* Power 3: A flexible statistical power analysis program for the social, behavioral, and biomedical sciences." In: *Behavior research methods* 39.2, pp. 175–191. DOI: `10.3758/BF03193146` (cit. on p. 43).

Fell, J., N. Axmacher (2011). "The role of phase synchronization in memory processes." In: *Nature Reviews Neuroscience* 12.2, pp. 105–118. DOI: `10.1038/nrn2979` (cit. on pp. 20, 22).

Fell, J., P. Klaver, K. Lehnertz, T. Grunwald, C. Schaller, C. E. Elger, G. Fernández (2001). "Human memory formation is accompanied by rhinal–hippocampal coupling and decoupling." In: *Nature Neuroscience* 4.12, pp. 1259–1264. DOI: `10.1038/nn759` (cit. on p. 18).

Fischl, B. (2012). "FreeSurfer." In: *NeuroImage* 62.2, pp. 774–781. DOI: `10.1016/j.neuroimage.2012.01.021` (cit. on p. 38).

Fregni, F., A. Pascual-Leone (2007). "Technology Insight: noninvasive brain stimulation in neurology—perspectives on the therapeutic potential of rTMS and tDCS." In: 3.7, pp. 383–393. DOI: `10.1038/ncpneuro0530` (cit. on p. 23).

Fries, P. (2015). "Rhythms for Cognition: Communication through Coherence." In: *Neuron* 88.1, pp. 220–235. DOI: `10.1016/j.neuron.2015.09.034` (cit. on p. 18).

Fujisawa, S., G. Buzsáki (2011). "A 4 Hz Oscillation Adaptively Synchronizes Prefrontal, VTA, and Hippocampal Activities." In: *Neuron* 72.1, pp. 153–165. DOI: `10.1016/j.neuron.2011.08.018` (cit. on p. 18).

Funahashi, S., K. Kubota (1994). "Working memory and prefrontal cortex." In: *Neuroscience research* 21.1, pp. 1–11. DOI: `10.1016/0168-0102(94)90063-9` (cit. on p. 60).

Ganis, G., M. Kutas (2003). "An electrophysiological study of scene effects on object identification." In: *Cognitive Brain Research* 16.2, pp. 123–144. DOI: `10.1016/S0926-6410(02)00244-6` (cit. on p. 16).

George, M. S., G. Aston-Jones (2009). "Noninvasive techniques for probing neurocircuitry and treating illness: vagus nerve stimulation (VNS), transcranial magnetic stimulation (TMS) and transcranial direct current stimulation (tDCS)." In: *Neuropsychopharmacology* 35.1, pp. 301–316. DOI: `10.1038/npp.2009.87` (cit. on p. 23).

George, M. S., T. A. Ketter, R. M. Post (1994). "Prefrontal cortex dysfunction in clinical depression." In: *Depression* 2.2, pp. 59–72. DOI: 10.1002/depr.3050020202 (cit. on p. 59).

George, M. S., S. H. Lisanby, D. Avery, W. M. McDonald, V. Durkalski, M. Pavlicova, et al. (2010). "Daily Left Prefrontal Transcranial Magnetic Stimulation Therapy for Major Depressive Disorder." In: *Archives of General Psychiatry* 67.5, p. 507. DOI: 10.1001/archgenpsychiatry.2010.46 (cit. on p. 11).

Gevins, A. (1997). "High-resolution EEG mapping of cortical activation related to working memory: effects of task difficulty, type of processing, and practice." In: *Cerebral Cortex* 7.4, pp. 374–385. DOI: 10.1093/cercor/7.4.374 (cit. on p. 19).

Gordon, P. C., P. Belardinelli, M. Stenroos, U. Ziemann, C. Zrenner (2022). "Prefrontal theta phase-dependent rTMS-induced plasticity of cortical and behavioral responses in human cortex." In: *Brain Stimulation* 15.2, pp. 391–402. DOI: 10.1016/j.brs.2022.02.006 (cit. on pp. 31, 79).

Gordon, P. C., S. Dörre, P. Belardinelli, M. Stenroos, B. Zrenner, U. Ziemann, C. Zrenner (June 2021). "Prefrontal Theta-Phase Synchronized Brain Stimulation With Real-Time EEG-Triggered TMS." In: *Frontiers in Human Neuroscience* 15. DOI: 10.3389/fnhum.2021.691821 (cit. on pp. 38–40, 48, 57, 79).

Grafman, J. (Dec. 1995). "Similarities and Distinctions among Current Models of Prefrontal Cortical Functions." In: *Annals of the New York Academy of Sciences* 769.1 Structure and, pp. 337–368. DOI: 10.1111/j.1749-6632.1995.tb38149.x (cit. on p. 13).

Groppa, S., A. Oliviero, A. Eisen, A. Quartarone, L. Cohen, V. Mall, et al. (2012). "A practical guide to diagnostic transcranial magnetic stimulation: Report of an IFCN committee." In: *Clinical Neurophysiology* 123.5, pp. 858–882. DOI: 10.1016/j.clinph.2012.01.010 (cit. on p. 37).

Guse, B., P. Falkai, O. Gruber, H. Whalley, L. Gibson, A. Hasan, et al. (2013). "The effect of long-term high frequency repetitive transcranial magnetic stimulation on working memory in schizophrenia and healthy controls—A randomized placebo-controlled, double-blind fMRI study." In: *Behavioural Brain Research* 237, pp. 300–307. DOI: 10.1016/j.bbr.2012.09.034 (cit. on p. 55).

Hallett, M. (2000). "Transcranial magnetic stimulation and the human brain." In: *Nature* 406.6792, pp. 147–150. DOI: 10.1038/35018000 (cit. on p. 13).

– (2007). "Transcranial Magnetic Stimulation: A Primer." In: *Neuron* 55.2, pp. 187–199. DOI: 10.1016/j.neuron.2007.06.026 (cit. on p. 23).

Hamada, M., N. Murase, A. Hasan, M. Balaratnam, J. C. Rothwell (2012). "The Role of Interneuron Networks in Driving Human Motor Cortical Plasticity." In: *Cerebral Cortex* 23.7, pp. 1593–1605. DOI: 10.1093/cercor/bhs147 (cit. on p. 12).

Hedges, L. V. (1981). "Distribution theory for Glass's estimator of effect size and related estimators." In: *journal of Educational Statistics* 6.2, pp. 107–128. DOI: 10.3102/10769986006002107 (cit. on p. 45).

Hill, A. T., P. B. Fitzgerald, K. E. Hoy (2016). "Effects of anodal transcranial direct current stimulation on working memory: a systematic review and meta-analysis of findings from healthy and neuropsychiatric populations." In: *Brain stimulation* 9.2, pp. 197–208. DOI: 10.1016/j.brs.2015.10.006 (cit. on p. 12).

Hsieh, L.-T., A. D. Ekstrom, C. Ranganath (2011). "Neural Oscillations Associated with Item and Temporal Order Maintenance in Working Memory." In: *Journal of Neuroscience* 31.30, pp. 10803–10810. DOI: 10.1523/JNEUROSCI.0828-11.2011 (cit. on p. 62).

Hsieh, L.-T., C. Ranganath (2014). "Frontal midline theta oscillations during working memory maintenance and episodic encoding and retrieval." In: *NeuroImage* 85, pp. 721–729. DOI: 10.1016/j.neuroimage.2013.08.003 (cit. on p. 19).

Huang, Y.-Z., M. J. Edwards, E. Rounis, K. P. Bhatia, J. C. Rothwell (2005). "Theta Burst Stimulation of the Human Motor Cortex." In: *Neuron* 45.2, pp. 201–206. DOI: 10.1016/j.neuron.2004.12.033 (cit. on p. 24).

Huerta, P. T., J. E. Lisman (1995). "Bidirectional synaptic plasticity induced by a single burst during cholinergic theta oscillation in CA1 in vitro." In: *Neuron* 15.5, pp. 1053–1063. DOI: 10.1016/0896-6273(95)90094-2 (cit. on pp. 12, 27).

Huerta, P. T., J. E. Lisman (1993). "Heightened synaptic plasticity of hippocampal CA1 neurons during a Cholinergically induced rhythmic state." In: *Nature* 364.6439, pp. 723–725. DOI: 10.1038/364723a0 (cit. on pp. 12, 27).

Ishii, R., K. Shinosaki, S. Ukai, T. Inouye, T. Ishihara, T. Yoshimine, et al. (1999). "Medial prefrontal cortex generates frontal midline theta rhythm." In: *NeuroReport* 10.4, pp. 675–679. DOI: 10.1097/00001756-199903170-00003 (cit. on p. 19).

Jenkinson, M., C. F. Beckmann, T. E. Behrens, M. W. Woolrich, S. M. Smith (2012). "FSL." In: *NeuroImage* 62.2, pp. 782–790. DOI: 10.1016/j.neuroimage.2011.09.015 (cit. on p. 38).

Jensen, O., J. E. Lisman (2005). "Hippocampal sequence-encoding driven by a cortical multi-item working memory buffer." In: *Trends in Neurosciences* 28.2, pp. 67–72. DOI: 10.1016/j.tins.2004.12.001 (cit. on p. 21).

Jensen, O., C. D. Tesche (2002). "Frontal theta activity in humans increases with memory load in a working memory task." In: *European Journal of Neuroscience* 15.8, pp. 1395–1399. DOI: 10.1046/j.1460-9568.2002.01975.x (cit. on pp. 19, 60).

Jutras, M. J., E. A. Buffalo (2010). "Synchronous neural activity and memory formation." In: *Current Opinion in Neurobiology* 20.2, pp. 150–155. DOI: 10.1016/j.conb.2010.02.006 (cit. on p. 20).

Kahana, M. J., R. Sekuler, J. B. Caplan, M. Kirschen, J. R. Madsen (1999). "Human theta oscillations exhibit task dependence during virtual maze navigation." In: *Nature* 399.6738, pp. 781–784. DOI: 10.1038/21645 (cit. on pp. 42, 57, 62).

Kane, M. J., A. R. A. Conway, T. K. Miura, G. J. H. Colflesh (2007). "Working memory, attention control, and the n-back task: A question of construct validity." In: *Journal of Experimental Psychology: Learning, Memory, and Cognition* 33.3, pp. 615–622. DOI: 10.1037/0278-7393.33.3.615 (cit. on p. 16).

Klimesch, W., M. Doppelmayr, H. Russegger, T. Pachinger (1996). "Theta band power in the human scalp EEG and the encoding of new information." In: *NeuroReport* 7.7, pp. 1235–1240. DOI: 10.1097/00001756-199605170-00002 (cit. on p. 19).

Klimesch, W., S. Hanslmayr, P. Sauseng, W. Gruber, C. Brozinsky, N. Kroll, et al. (2005). "Oscillatory EEG Correlates of Episodic Trace Decay." In: *Cerebral Cortex* 16.2, pp. 280–290. DOI: 10.1093/cercor/bhi107 (cit. on p. 19).

Konorski, J. (1948). *Conditioned reflexes and neuron organization.* Cambridge University Press (cit. on p. 20).

Larson, J., E. Munkácsy (2015). "Theta-burst LTP." In: *Brain Research* 1621, pp. 38–50. DOI: 10.1016/j.brainres.2014.10.034 (cit. on p. 25).

Lawrence, A. (1998). "Evidence for specific cognitive deficits in preclinical Huntington's disease." In: *Brain* 121.7, pp. 1329–1341. DOI: 10.1093/brain/121.7.1329 (cit. on p. 15).

Lefaucheur, J.-P., A. Aleman, C. Baeken, D. H. Benninger, J. Brunelin, V. D. Lazzaro, et al. (2020). "Evidence-based guidelines on the therapeutic use of repetitive transcranial magnetic stimulation (rTMS): An update (2014–2018)." In: *Clinical Neurophysiology* 131.2, pp. 474–528. DOI: 10.1016/j.clinph.2019.11.002 (cit. on p. 11).

Lopez-Alonso, V., B. Cheeran, D. Rio-Rodriguez, M. Fernandez-del-Olmo (May 2014). "Inter-individual Variability in Response to Non-invasive Brain Stimulation Paradigms." In: *Brain Stimulation* 7.3, pp. 372–380. DOI: 10.1016/j.brs.2014.02.004 (cit. on p. 12).

McLoughlin, G., M. Gyurkovics, J. Palmer, S. Makeig (2021). "Midfrontal Theta Activity in Psychiatric Illness: An Index of Cognitive Vulnerabilities Across Disorders." In: *Biological psychiatry*. DOI: 10.1016/j.biopsych.2021.08.020 (cit. on p. 19).

– (2022). "Midfrontal Theta Activity in Psychiatric Illness: An Index of Cognitive Vulnerabilities Across Disorders." In: *Biological Psychiatry* 91.2, pp. 173–182. DOI: 10.1016/j.biopsych.2021.08.020 (cit. on p. 15).

Miller, E. K., J. D. Cohen (2001). "An Integrative Theory of Prefrontal Cortex Function." In: *Annual Review of Neuroscience* 24.1, pp. 167–202. DOI: 10.1146/annurev.neuro.24.1.167 (cit. on pp. 15, 61).

Miller, M. H., J. Orbach (1972). "Retention of spatial alternation following frontal lobe resections in stump-tailed macaques." In: *Neuropsychologia* 10.3, pp. 291–298. DOI: 10.1016/0028-3932(72)90020-6 (cit. on p. 14).

Mulkey, R. M., R. C. Malenka (1992). "Mechanisms underlying induction of homosynaptic long-term depression in area CA1 of the hippocampus." In: *Neuron* 9.5, pp. 967–975. DOI: 10.1016/0896-6273(92)90248-C (cit. on p. 20).

Müller-Dahlhaus, F., A. Vlachos (2013). "Unraveling the cellular and molecular mechanisms of repetitive magnetic stimulation." In: *Frontiers in Molecular Neuroscience* 6. DOI: 10.3389/fnmol.2013.00050 (cit. on p. 13).

Nachev, P., G. Rees, A. Parton, C. Kennard, M. Husain (2005). "Volition and Conflict in Human Medial Frontal Cortex." In: *Current Biology* 15.2, pp. 122–128. DOI: `10.1016/j.cub.2005.01.006` (cit. on p. 60).

O'Reardon, J. P., H. B. Solvason, P. G. Janicak, S. Sampson, K. E. Isenberg, Z. Nahas, et al. (2007). "Efficacy and Safety of Transcranial Magnetic Stimulation in the Acute Treatment of Major Depression: A Multisite Randomized Controlled Trial." In: *Biological Psychiatry* 62.11, pp. 1208–1216. DOI: `10.1016/j.biopsych.2007.01.018` (cit. on p. 12).

Oldfield, R. (1971). "The assessment and analysis of handedness: The Edinburgh inventory." In: *Neuropsychologia* 9.1, pp. 97–113. DOI: `10.1016/0028-3932(71)90067-4` (cit. on p. 32).

Onton, J., A. Delorme, S. Makeig (2005). "Frontal midline EEG dynamics during working memory." In: *NeuroImage* 27.2, pp. 341–356. DOI: `10.1016/j.neuroimage.2005.04.014` (cit. on p. 19).

Oostenveld, R., P. Praamstra (2001). "The five percent electrode system for high-resolution EEG and ERP measurements." In: *Clinical Neurophysiology* 112.4, pp. 713–719. DOI: `10.1016/s1388-2457(00)00527-7` (cit. on p. 36).

Pavlides, C., Y. J. Greenstein, M. Grudman, J. Winson (1988). "Long-term potentiation in the dentate gyrus is induced preferentially on the positive phase of theta-rhythm." In: *Brain Research* 439.1-2, pp. 383–387. DOI: `10.1016/0006-8993(88)91499-0` (cit. on p. 27).

Payne, L., J. Kounios (2009). "Coherent oscillatory networks supporting short-term memory retention." In: *Brain Research* 1247, pp. 126–132. DOI: `10.1016/j.brainres.2008.09.095` (cit. on p. 20).

Penney, C. G. (1989). "Modality effects in short-term verbal memory." In: *Psychological Bulletin* 82.1, pp. 68–84. DOI: `10.1037/h0076166` (cit. on p. 16).

Phillips, M. L., C. D. Ladouceur, W. C. Drevets (2008). "A neural model of voluntary and automatic emotion regulation: implications for understanding the pathophysiology and neurodevelopment of bipolar disorder." In: *Molecular Psychiatry* 13.9, pp. 833–857. DOI: `10.1038/mp.2008.65` (cit. on pp. 15, 61).

Polti, I., B. Martin, V. van Wassenhove (2018). "The effect of attention and working memory on the estimation of elapsed time." In: *Scientific Reports* 8.1. DOI: `10.1038/s41598-018-25119-y` (cit. on p. 44).

Raghavachari, S., M. J. Kahana, D. S. Rizzuto, J. B. Caplan, M. P. Kirschen, B. Bourgeois, et al. (2001). "Gating of Human Theta Oscillations by a Working Memory Task." In: *The Journal of Neuroscience* 21.9. Theta linked to working memory, pp. 3175–3183. DOI: `10.1523/JNEUROSCI.21-09-03175.2001` (cit. on p. 62).

Reppermund, S., M. Ising, S. Lucae, J. Zihl (2008). "Cognitive impairment in unipolar depression is persistent and non-specific: further evidence for the final common pathway disorder hypothesis." In: *Psychological Medicine* 39.4, pp. 603–614. DOI: `10.1017/S003329170800411X` (cit. on p. 15).

Ridding, M. C., U. Ziemann (2010). "Determinants of the induction of cortical plasticity by non-invasive brain stimulation in healthy subjects." In: *The Journal of Physiology* 588.13, pp. 2291–2304. DOI: `10.1113/jphysiol.2010.190314` (cit. on p. 12).

Rutishauser, U., I. B. Ross, A. N. Mamelak, E. M. Schuman (2010). "Human memory strength is predicted by theta-frequency phase-locking of single neurons." In: *Nature* 464.7290, pp. 903–907. DOI: `10.1038/nature08860` (cit. on p. 18).

Sarnthein, J., H. Petsche, P. Rappelsberger, G. L. Shaw, A. von Stein (1998). "Synchronization between prefrontal and posterior association cortex during human working memory." In: *Proceedings of the National Academy of Sciences* 95.12, pp. 7092–7096. DOI: `10.1073/pnas.95.12.7092` (cit. on p. 19).

Sato, N., Y. Yamaguchi (2007). "Theta synchronization networks emerge during human object–place memory encoding." In: *NeuroReport* 18.5, pp. 419–424. DOI: `10.1097/WNR.0b013e3280586760` (cit. on p. 20).

Sauseng, P., W. Klimesch, K. F. Heise, W. R. Gruber, E. Holz, A. A. Karim, et al. (2009). "Brain Oscillatory Substrates of Visual Short-Term Memory Capacity." In: *Current Biology* 19.21, pp. 1846–1852. DOI: `10.1016/j.cub.2009.08.062` (cit. on p. 22).

Schack, B., W. Klimesch, P. Sauseng (2005). "Phase synchronization between theta and upper alpha oscillations in a working memory task." In: *International Journal of Psychophysiology* 57.2, pp. 105–114. DOI: `10.1016/j.ijpsycho.2005.03.016` (cit. on p. 22).

Schacter, D. L. (1977). "EEG theta waves and psychological phenomena: A review and analysis." In: *Biological Psychology* 5.1, pp. 47–82. DOI: `10.1016/0301-0511(77)90028-X` (cit. on p. 19).

Siapas, A. G., E. V. Lubenov, M. A. Wilson (2005). "Prefrontal Phase Locking to Hippocampal Theta Oscillations." In: *Neuron* 46.1, pp. 141–151. DOI: `10.1016/j.neuron.2005.02.028` (cit. on p. 19).

Siegle, J. H., M. A. Wilson (2014). "Enhancement of encoding and retrieval functions through theta phase-specific manipulation of hippocampus." In: *eLife* 3, e03061. DOI: `10.7554/eLife.03061` (cit. on p. 56).

Sternberg, S. (1966). "High-Speed Scanning in Human Memory." In: *Science* 153.3736, pp. 652–654. DOI: `10.1126/science.153.3736.652` (cit. on pp. 16, 42).

Sternberg, S. (1969). "Memory-scanning: Mental processes revealed by reaction-time experiments." In: *American scientist* 57.4, pp. 421–457 (cit. on p. 16).

Tsujimoto, T., H. Shimazu, Y. Isomura, K. Sasaki (2010). "Theta Oscillations in Primate Prefrontal and Anterior Cingulate Cortices in Forewarned Reaction Time Tasks." In: *Journal of Neurophysiology* 103.2, pp. 827–843. DOI: `10.1152/jn.00358.2009` (cit. on p. 62).

Ullsperger, M., D. von Cramon (2001). "Subprocesses of Performance Monitoring: A Dissociation of Error Processing and Response Competition Revealed by Event-Related fMRI and ERPs." In: *NeuroImage* 14.6, pp. 1387–1401. DOI: `10.1006/nimg.2001.0935` (cit. on p. 60).

Veen, B. V., W. V. Drongelen, M. Yuchtman, A. Suzuki (1997). "Localization of brain electrical activity via linearly constrained minimum variance spatial filtering." In: *IEEE Transactions on Biomedical Engineering* 44.9, pp. 867–880. DOI: `10.1109/10.623056` (cit. on p. 38).

Venkatraman, V., A. G. Rosati, A. A. Taren, S. A. Huettel (2009). "Resolving Response, Decision, and Strategic Control: Evidence for a Functional Topography in Dorsomedial Prefrontal Cortex." In: *Journal of Neuroscience* 29.42, pp. 13158–13164. DOI: `10.1523/JNEUROSCI.2708-09.2009` (cit. on pp. 15, 61).

Vlachos, A., F. Muller-Dahlhaus, J. Rosskopp, M. Lenz, U. Ziemann, T. Deller (2012). "Repetitive Magnetic Stimulation Induces Functional and Structural Plasticity of Excitatory Postsynapses in Mouse Organotypic Hippocampal Slice Cultures." In: *Journal of Neuroscience* 32.48, pp. 17514–17523. DOI: `10.1523/JNEUROSCI.0409-12.2012` (cit. on p. 24).

Windhoff, M., A. Opitz, A. Thielscher (2011). "Electric field calculations in brain stimulation based on finite elements: An optimized processing pipeline for the generation and usage of accurate individual head models." In: *Human Brain Mapping* 34.4, pp. 923–935. DOI: `10.1002/hbm.21479` (cit. on p. 38).

Wu, A. D., F. Fregni, D. K. Simon, C. Deblieck, A. Pascual-Leone (2008). "Noninvasive brain stimulation for Parkinson's disease and dystonia." In: *Neurotherapeutics* 5.2, pp. 345–361. DOI: `10.1016/j.nurt.2008.02.002` (cit. on p. 15).

Ziemann, U., W. Paulus, M. A. Nitsche, A. Pascual-Leone, W. D. Byblow, A. Berardelli, et al. (2008). "Consensus: Motor cortex plasticity protocols." In: *Brain Stimulation* 1.3, pp. 164–182. DOI: `10.1016/j.brs.2008.06.006` (cit. on p. 24).

Ziemann, U., J. Reis, P. Schwenkreis, M. Rosanova, A. Strafella, R. Badawy, F. Müller-Dahlhaus (2015). "TMS and drugs revisited 2014." In: *Clinical Neurophysiology* 126.10, pp. 1847–1868. ISSN: 1388-2457. DOI: `10.1016/j.clinph.2014.08.028` (cit. on p. 12).

Zrenner, C., P. Belardinelli, D. Desideri, U. Ziemann (2017a). "Brain-state triggered 100 Hz triple-pulse TMS differentially induces LTP- or LTD-like effects depending on synchrony with negative or positive peak phase of endogenous sensorimotor mu-alpha oscillations." In: *Clinical Neurophysiology* 128.3, e159. DOI: `10.1016/j.clinph.2016.10.411` (cit. on p. 27).

– (2017b). "Phase of brain oscillations determines the direction of induced plasticity in real-time EEG-triggered TMS." In: *Brain Stimulation* 10.2, p. 429. DOI: `10.1016/j.brs.2017.01.277` (cit. on p. 27).

Zrenner, C., D. Desideri, P. Belardinelli, U. Ziemann (2018). "Real-time EEG-defined excitability states determine efficacy of TMS-induced plasticity in human motor cortex." In: *Brain Stimulation* 11.2, pp. 374–389. DOI: `10.1016/j.brs.2017.11.016` (cit. on pp. 56, 57).

Zrenner, C., D. Galevska, J. O. Nieminen, D. Baur, M.-I. Stefanou, U. Ziemann (2020). "The shaky ground truth of real-time phase estimation." In: *NeuroImage* 214, p. 116761. DOI: `10.1016/j.neuroimage.2020.116761` (cit. on pp. 57, 62).

8 Declaration of Candidates own Contribution

The work was carried out at the Hertie institute for clinical brain research under the supervision of Prof. Dr. Ulf Ziemann.

The study was designed in collaboration with Dr. Pedro Gordon (postdoc) and Dr. Christoph Zrenner (postdoc). The development of the applied method of EEG-triggered stimulation was done by Pedro Gordon and Christoph Zrenner. The selection and configuration of the working memory task were done by me.

The experiments were conducted by me in collaboration with Pedro Gordon, Dragana Galevska (research assistant), and Anna Kempf (project coordinator).

The statistical analysis was performed independently by me, except for the analysis of the accuracy of the phase detection algorithm, which was performed by Pedro Gordon.

I assure that I have written this doctoral thesis independently and that I have not used any sources other than those indicated by me.

9 Publications

Parts of this work have been published in the form of the following scientific articles:

Gordon, P. C., S. Dörre, P. Belardinelli, M. Stenroos, B. Zrenner, U. Ziemann, and C. Zrenner (June 2021). "Prefrontal Theta-Phase Synchronized Brain Stimulation With Real-Time EEG-Triggered TMS." in: *Frontiers in Human Neuroscience* 15. DOI: 10.3389/fnhum.2021.691821

Gordon, P. C., P. Belardinelli, M. Stenroos, U. Ziemann, and C. Zrenner (2022). "Prefrontal theta phase-dependent rTMS-induced plasticity of cortical and behavioral responses in human cortex." In: *Brain Stimulation* 15.2, pp. 391–402. DOI: 10.1016/j.brs.2022.02.006

10 Acknowledgements

At this point, I would like to express my sincere thanks to all of those who have contributed to the success of this work:

First and foremost, I would like to thank Prof. Dr. Ulf Ziemann for providing the interesting topic as well as for his constructive criticism to improve this thesis.

Also, I would like to thank Dr. Christoph Zrenner and Dr. Pedro Gordon, who supervised the experiment and this thesis. Thank you for supporting me with productive conversations, friendly patient advice, and your constant availability.

I would also like to thank all the subjects for their participation in this study, as well as anyone helping in conducting the experiment.

Last but not least, I would like to thank my family and friends for their motivation, support, and corrections of the manuscript. In particular, I would like to thank Alexander Van Craen for his encouragement and patience and for tirelessly solving LaTeX problems.